Journal of Medicinal Chemistry

Article

pubs.acs.org/jmc

Novel Cyclopentadienyl Tricarbonyl ^{99m}Tc Complexes Containing 1-Piperonylpiperazine Moiety: Potential Imaging Probes for Sigma-1 Receptors

Xia Wang,[†] Dan Li,[†] Winnie Deuther-Conrad,[‡] Jie Lu,[†] Ying Xie,[§] Bing Jia,[⊥] Mengchao Cui,[†] Jörg Steinbach,[‡] Peter Brust,[‡] Boli Liu,[†] and Hongmei Jia*[,†]

[†]Key Laboratory of Radiopharmaceuticals (Beijing Normal University), Ministry of Education, College of Chemistry, Beijing Normal University, Beijing 100875, China

[‡]Institute of Radiopharmaceutical Cancer Research/Department of Neuroradiopharmaceuticals, Helmholtz-Zentrum Dresden-Rossendorf, 04318 Leipzig, Germany

[§]Department of Pharmaceutics, School of Pharmaceutical Sciences, Peking University, Beijing 100191, China

[⊥]Department of Radiation Medicine, School of Basic Medical Sciences, Peking University, Beijing 100191, China

Supporting Information

ABSTRACT: We report the design, synthesis, and evaluation of a series of novel cyclopentadienyl tricarbonyl ^{99m}Tc complexes as potent σ_1 receptor radioligands. Rhenium compounds 3-(4-(1,3-benzodioxol-5-ylmethyl)piperazin-1-yl)-propylcarbonylcyclopentadienyl tricarbonyl rhenium (**10a**) and 4-(4-(1,3-benzodioxol-5-ylmethyl)piperazin-1-yl)-butylcarbonylcyclopentadienyl tricarbonyl rhenium (**10b**) possessed high in vitro affinity for σ_1 receptors and moderate to high selectivity for σ_2 receptors and the vesicular acetylcholine transporter. Biodistribution studies in mice demonstrated high initial brain uptake for corresponding ^{99m}Tc derivatives [^{99m}Tc]**23** and [^{99m}Tc]**24** of 2.94 and 2.13% injected dose (ID)/g, respectively, at 2 min postinjection. Pretreatment of haloperidol significantly reduced the radiotracer accumulation of [^{99m}Tc]**23** or [^{99m}Tc]**24** in the brain. Studies of the cellular uptake of [^{99m}Tc]**23** in C6 and DU145 tumor cells demonstrated a reduction of accumulation by incubation with haloperidol, 1-(3,4-dimethoxyphenethyl)-4-(3-phenylpropyl)piperazine (SA4503), or 1,3-di-*o*-tolyl-guanidine (DTG). Furthermore, blocking studies in C6 glioma-bearing mice confirmed the specific binding of [^{99m}Tc]**23** to σ_1 receptors in the tumor.

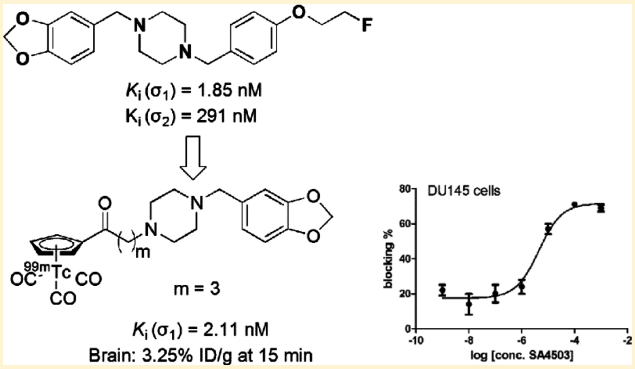

INTRODUCTION

The sigma-1 (σ_1) receptor is a unique "ligand-operated receptor chaperone".[1] It consists of 223 amino acids and is assumed to contain two transmembrane segments.[2,3] It is believed to be involved in the regulation of various signal transduction processes, endoplasmic reticulum (ER) stress, cellular redox processes, cellular survival, and synaptogenesis in the central nervous system (CNS).[4−6] There is strong evidence for the involvement of σ_1 receptors in the pathophysiology of a number of brain diseases, including drug addiction, depression, Alzheimer's disease (AD), and Parkinson's disease (PD).[4,5,7−11] Moreover, σ_1 receptors are overexpressed in many human tumors, and they play a significant role in cancer biology.[12−16] Therefore, radiotracers with appropriate affinity and high specificity for σ_1 receptors could be useful in the early diagnosis of various brain diseases and tumors using noninvasive imaging techniques such as positron emission tomography (PET) and single photon emission computed tomography (SPECT).

Over the past decade, many PET and SPECT radiotracers for σ_1 receptors have been reported.[17] However, no suitable radiotracers for σ_1 receptor imaging have been used in clinic to date. Among the three radiotracers investigated thus far in humans, [^{18}F]1-(3-fluoropropyl)-4-((4-cyanophenoxy)methyl)-piperidine ([^{18}F]FPS) and (*E*)-[^{123}I]1-(3-iodoallyl)-4-((4-cyanophenoxy)methyl)piperidine ([^{123}I]TPCNE) displayed irreversible kinetics in the brain.[18,19] [^{11}C]1-(3,4-dimethoxyphenethyl)-4-(3-phenylpropyl)piperazine ([^{11}C]SA4503), the first useful PET imaging agent, has been used for the evaluation of σ_1 receptor occupancy by therapeutic drugs in the human brain.[20−22] However, the use of [^{11}C]SA4503 needs an on-site cyclotron due to the short half-life of ^{11}C ($t_{1/2}$ = 20 min). Currently, due to the widespread use of SPECT, the almost ideal nuclear properties of ^{99m}Tc, and relatively low costs for

Received: June 22, 2014

   dx.doi.org/10.1021/jm5009488 | *J. Med. Chem.* XXXX, XXX, XXX−XXX

SPECT imaging, ^{99m}Tc is the most widely used radionuclide, employed in approximately 80% of all nuclear medicine procedures. Thus, ^{99m}Tc-labeled radiotracers targeting σ_1 receptors are expected to provide simple, convenient, and low-cost diagnostic tools for the investigation of the σ_1 receptor status in a wide range of human diseases.

The basic requirements for a useful radiotracer for σ_1 receptor imaging in the CNS include high binding affinity for σ_1 receptors and selectivity toward other potential targets, high brain uptake, high specific binding to σ_1 receptors, and low nonspecific binding in vivo. If there is any radiometabolite in the blood, it should not be able to cross the blood–brain barrier. Unlike the ^{11}C- or radiohalogen-labeled radiotracers, ^{99m}Tc-labeled imaging agents cannot be straightforwardly derived from a suitable σ_1 receptor ligand. ^{99m}Tc is a transition metal and requires a chelate for complexation. A fundamental challenge lies in the acceptable integration of ^{99m}Tc-chelate unit into the σ_1 receptor ligand. Moreover, the low brain uptake is still the bottleneck in the development of ^{99m}Tc-labeled CNS receptor radiotracers until now. To meet the above-mentioned requirements for σ_1 receptor radiotracers, three building blocks, including a receptor-binding moiety, a small ^{99m}Tc-chelate unit, and a suitable linker, need to be carefully considered for the design of ^{99m}Tc-labeled radiotracers targeting σ_1 receptors.[23] The structures of ^{99m}Tc-labeled σ_1 receptor radiotracers developed recently are presented in Figure 1. Among these,

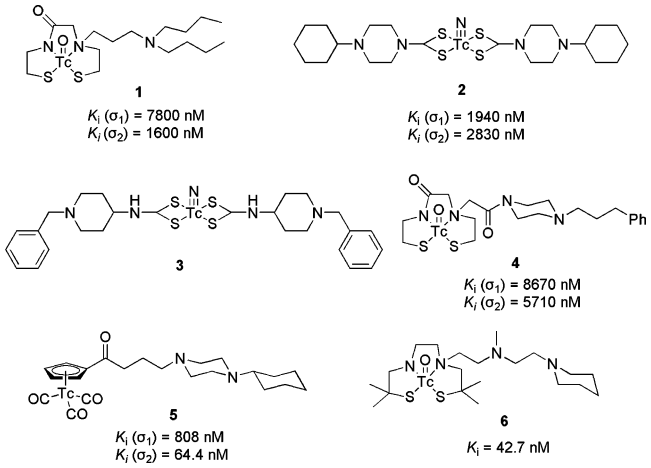

Figure 1. Structures of ^{99m}Tc-labeled σ_1 receptor radiotracers developed recently.

no in vitro affinity data were reported for **3**.[24] Complexes **1**,[25] **2**,[26] **4**,[27] and **5**[28] displayed micromolar affinity for σ_1 receptors. For compound **6**, the subtype-independent binding affinity estimated by [^{3}H]1,3-di-*o*-tolyl-guanidine ([^{3}H]DTG) displacement studies was moderate (K_i = 42.7 nM).[29] Thus, no potential ^{99m}Tc-labeled σ_1 receptor imaging agent has been developed so far.

Recently, the neutral and lipophilic "piano stool" organometallic core, [(Cp-R)M(CO)$_3$] (M = ^{99m}Tc, Re), has become particularly attractive due to its stability and compactness.[30] Our previous work regarding σ_2 receptor ligands demonstrated that the replacement of the 1,2,3,4-tetrahydronaphthalene group in 1-cyclohexyl-4-[3-(5-methoxy-1,2,3,4-tetrahydronaphthalen-1-yl)-propyl]piperazine (PB28) with the [(Cp-R)M(CO)$_3$] (M = ^{99m}Tc, Re) unit retained high affinity for the target.[28] Therefore, it seems reasonable to design novel ^{99m}Tc-labeled σ_1 receptor-targeting radiotracers by using the [(Cp-R)^{99m}Tc(CO)$_3$] core. Previously, we reported the high affinity ($K_i(\sigma_1)$ = 1.85 nM) and high subtype selectivity ($K_i(\sigma_2)/K_i(\sigma_1)$ = 157) of [^{18}F]1-(1,3-benzodioxol-5-ylmethyl)-4-(4-(2-fluoroethoxy)benzyl)piperazin ([^{18}F]**7**) for σ_1 receptors in vitro as well as high initial brain uptake and specific binding to σ_1 receptors in vivo.[31] In the present study, we used [^{18}F]**7** as a lead compound to design novel [(Cp-R)M(CO)$_3$] (M = ^{99m}Tc, Re) complexes as potent σ_1 receptor ligands through an integrated approach. Our design concept is shown in Figure 2. We replaced the benzyl moiety in compound **7** with the [(Cp-R)M(CO)$_3$] unit and connected it to the 1-piperonylpiperazine moiety via a proper linker. We introduced a carbonyl or amide group to meet the requirement for an electron-withdrawing group on the [(Cp-R)^{99m}Tc(CO)$_3$] substituent that would allow the double ligand transfer (DLT) reaction to proceed efficiently for the synthesis of the [(Cp-R)^{99m}Tc(CO)$_3$] complex from the corresponding ferrocene precursor. In addition, the introduction of a carbonyl or amide group could decrease the lipophilicity of the complex and consequently decrease the nonspecific binding in vivo. According to the pharmacophore model proposed by Glennon, σ_1 receptor ligands possess one basic nitrogen atom flanked by two hydrophobic regions.[32] This integrated strategy of replacing a hydrophobic region with the lipophilic ^{99m}Tc-chelate unit should minimize the change in molecular size and might retain affinity for σ_1 receptors. In this study, we report the synthesis of novel [(Cp-R)M(CO)$_3$] (M = ^{99m}Tc, Re) complexes, and we evaluated them as potent σ_1 receptor ligands through biodistribution and blocking studies in mice, cellular uptake studies in tumor cells, blocking studies in tumor-bearing mice, and radiometabolite studies.

RESULTS

Chemistry. For the biological characterization of the ^{99m}Tc complexes, we prepared the corresponding rhenium complexes as shown in Scheme 1. Intermediates **8a–8c** were synthesized according to literature methods.[28] Friedel–Crafts monoacylation of cyclopentadienyl tricarbonyl rhenium with bromide-substituted anoyl chloride produced the corresponding compounds **8a–8c** in high yields. N-Alkylation of 1-piperonylpiperazine (**9**) with **8a**, **8b**, and **8c** provided **10a**, **10b**, and **10c**, respectively.

Compounds **12** and **13** were synthesized according to the method reported previously.[33] 1-Piperonylpiperazine (**9**)

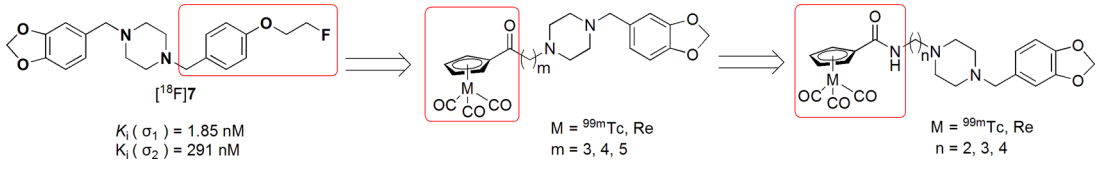

Figure 2. Design concept of novel [(Cp-R)M(CO)$_3$] (M = ^{99m}Tc, Re) complexes as potent σ_1 receptor ligands.

dx.doi.org/10.1021/jm5009488 | J. Med. Chem. XXXX, XXX, XXX–XXX

Scheme 1. Synthetic Routes for Rhenium Compounds 10a−10c and 16a−16c[a]

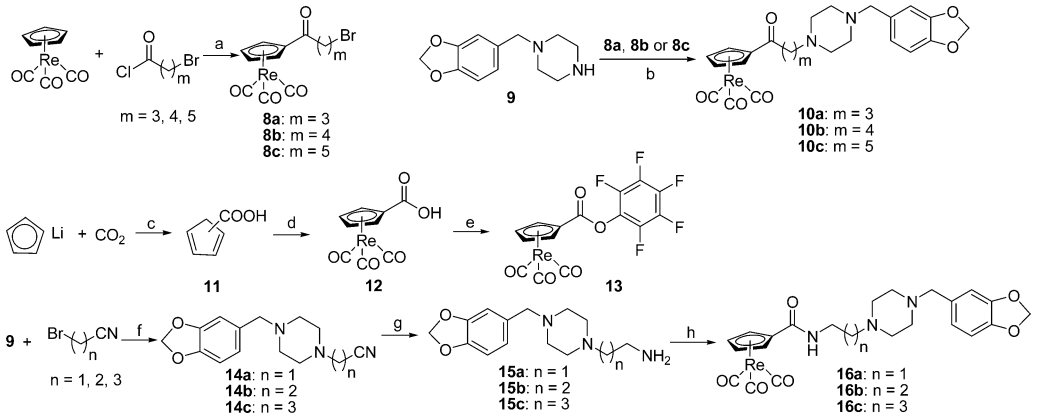

[a]Reagents and conditions: (a) anhydrous CH_2Cl_2, anhydrous $AlCl_3$, 0 °C to rt, 71% for **8a**, 75% for **8b**, 87% for **8c**; (b) toluene, KI, Et_3N, 115 °C, 16% for **10a**, 22% for **10b**, 46% for **10c**; (c) (i) anhydrous THF, −30 °C, (ii) 20% HCl, 14%; (d) $Re_2(CO)_{10}$, mesitylene, 190 °C, 95%; (e) pentafluorophenyl trifluoroacetate, pyridine, DMF, N_2, rt, 53%; (f) CH_2Cl_2, Et_3N, rt, 43% for **14a**, 74% for **14b**, 70% for **14c**; (g) THF, $LiAlH_4$, diethyl ether, 32% for **15a**, 40% for **15b**, 45% for **15c**; (h) **13**, anhydrous DMF, Et_3N, rt, 40% for **16a**, 92% for **16b**, 61% for **16c**.

reacted with bromine-substituted nitrile to provide the corresponding **14a−14c**. Reduction of **14a−14c** using $LiAlH_4$ afforded **15a−15c**, respectively. The synthetic method for compound **15a** in this paper is different from that reported in the literature.[34] The activated ester **13** reacted with **15a**, **15b**, or **15c** at room temperature to provide target complexes **16a**, **16b**, or **16c**, respectively.

The target compounds (**10a−10c** and **16a−16c**) were characterized by ^{1}H NMR, ^{13}C NMR, and high-resolution mass spectrometry (HRMS) with the purities of ≥95% as shown in the Supporting Information.

In Vitro Radioligand Competition Studies. The affinities of the novel cyclopentadienyl tricarbonyl rhenium complexes for the σ_1 and σ_2 receptors and for the vesicular acetylcholine transporter (VAChT) were determined with radioligand competition experiments as previously reported.[27,35] The binding assays used (+)-[^{3}H]pentazocine for the σ_1 receptors, [^{3}H]DTG in the presence of 10 μM dextrallorphan for the σ_2 receptors, and (−)-[^{3}H]vesamicol for VAChT. The results are listed in Table 1. In general, cyclopentadienyl tricarbonyl rhenium complexes and ferrocene precursors except for **10c** preferred to bind to σ_1 receptors. The amide-substituted complexes (**16a−16c**, **22**) displayed moderate affinity for σ_1 receptors with K_i values of 50.6−65.0 nM and low affinity for σ_2 receptors, thus giving them moderate subtype selectivity (9.70−14.0) for σ_1 receptors. The carbonyl-substituted complexes **10a**, **10b**, and **20** displayed very high σ_1 binding affinities, with K_i values ranging from 2.11 nM for **10a** and 4.90 nM for **10b** to 7.67 nM for **20**. Moreover, these compounds displayed moderate to low σ_2 binding affinities. In particular, **10a** displayed comparable affinity and subtype selectivity for σ_1 receptors to SA4503. **10b** displayed comparable affinity and even higher subtype selectivity (2-fold) for σ_1 receptors to SA4503. These results indicate that the nanomolar affinity and moderate to high subtype selectivity for σ_1 receptors could be maintained by replacing the phenyl ring with a cyclopentadienyl tricarbonyl rhenium unit or ferrocene (**10a** vs **7**, **10b** vs **7**, **20** vs **7**). However, if the number of carbon atoms between the carbonyl group and the 1-piperonylpiperazine moiety was increased to 5, decreased affinity and subtype selectivity for σ_1 receptors was observed (**10c** vs**10a**, **10c** vs**10b**), indicating that the carbon linker length affected the affinity for σ_1 receptors.

Table 1. Binding Affinities of Cyclopentadienyl Tricarbonyl Rhenium Complexes for σ_1 and σ_2 Receptors[a]

compd	K_i (σ_1) (nM)	K_i (σ_2) (nM)	$K_i(\sigma_2)/K_i(\sigma_1)$
7[b]	1.85 ± 1.59	291 ± 111	157
10a	2.11 ± 1.36	30.7 ± 3.83	14.5
10b	4.90 ± 1.01	160 ± 108	32.7
10c	239 ± 31.8	94.1 ± 6.51	0.39
16a	56.5 ± 17.8	548 ± 55.2	9.70
16b	65.0 ± 53.8	907 ± 191	14.0
16c	50.6 ± 10.1	610 ± 154	12.1
20	7.67 ± 2.10	311 ± 95.5	40.5
22	54.8 ± 4.11	377 ± 38.6	6.88
SA4503	3.33 ± 0.12	50.7 ± 1.27	15.2

[a]Values are means ± standard deviation (SD) of three experiments performed in triplicate. [b]From ref 31.

Considering the high affinity and subtype selectivity of compounds **10a** and **10b** for σ_1 receptors, both were further tested for their affinity for VAChT. Compound **10a** displayed low affinity for VAChT (K_i = 1155 ± 250 nM) and was thus characterized by an excellent selectivity for σ_1 receptors (K_i(VAChT)/K_i(σ_1) = 547). Complex **10b** displayed moderate affinity for VAChT (K_i = 35.5 ± 25.7 nM). To assess the kinetics of the corresponding radiotracers, we prepared the corresponding ^{99m}Tc-labeled complexes of **10a** and **10b** for further evaluation.

Radiolabeling. The synthetic routes for the corresponding ferrocene precursors were similar to those of the rhenium complexes (Scheme 2). Acylation of ferrocene with 4-bromobutanoyl chloride or 5-bromopentanoyl chloride provided compounds **17** and **18**, respectively, according to the method reported previously.[36] Alkylation of **9** with **17** or **18** using triethylamine as a base yielded **20** or **21**, respectively. Ferrocenecarboxylic acid reacted with pentafluorophenyl trifluoroacetate to obtain compound **19** in a synthesis different from that reported in the literature.[37] Condensation of **15a** with **19** resulted in the ferrocene precursor **22**.

The synthesis of [^{99m}Tc]**23−25** was accomplished according to published methods with minor modifications (Scheme 3).[28,38] The formation of the desired ^{99m}Tc-labeled radiotracers

dx.doi.org/10.1021/jm5009488 | J. Med. Chem. XXXX, XXX, XXX−XXX

Scheme 2. Synthetic Routes for Precursors 20–22[a]

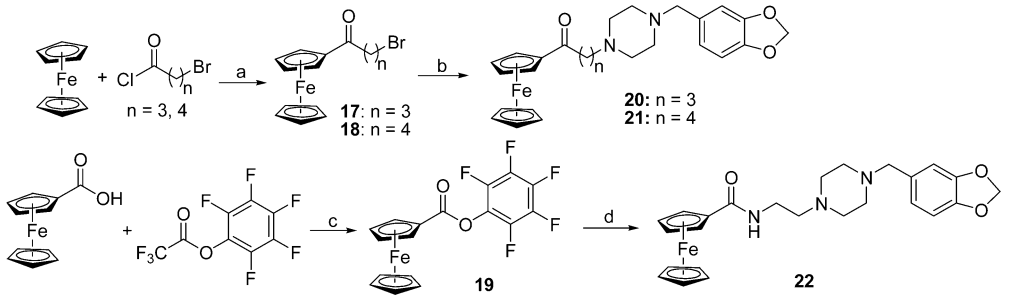

[a]Reagents and conditions: (a) anhydrous CH_2Cl_2, anhydrous $AlCl_3$, 0 °C to rt, 72% for **17**, 79% for **18**; (b) **9**, toluene, KI, Et_3N, 115 °C, 60% for **20**, 62% for **21**; (c) anhydrous DMF, pyridine, rt, 57%; (d) **15a**, anhydrous DMF, Et_3N, rt, 42%.

Scheme 3. Synthesis of [^{99m}Tc]23–25 from the Corresponding Ferrocene Precursors[a]

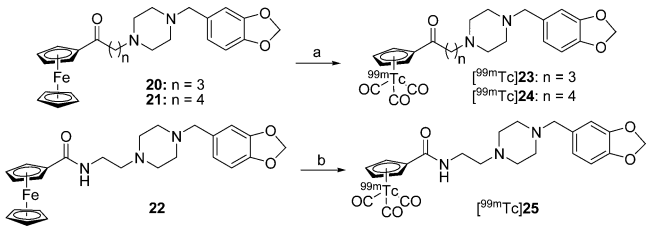

[a]Reagents and conditions: (a) $^{99m}TcO_4^-$, $Mn(CO)_5Br$, DMF, 140 °C, 50–60%; (b) $^{99m}TcO_4^-$, $Mn(CO)_5Br$, DMF, 160 °C, 50–60%.

from the corresponding ferrocene precursors was accomplished via the DLT reaction at 140 °C (or 160 °C) for 1 h. After purification by semipreparative high performance liquid chromatography (HPLC), [^{99m}Tc]**23** (n = 6), [^{99m}Tc]**24** (n = 3), and [^{99m}Tc]**25** (n = 3) were obtained in approximately 50–60% radiochemical yields (decay-corrected) with a radiochemical purity of >99%.

Evaluation of Radiolabeled Complexes. *Lipophilicity.* The apparent distribution coefficients of ^{99m}Tc-labeled complexes were determined by measuring their distribution between 1-octanol and 0.05 mol·L^{-1} sodium phosphate buffer at pH 7.4 as previously reported.[39] The log D values of [^{99m}Tc]**23–25** are 2.24 ± 0.02, 2.68 ± 0.01, and 3.09 ± 0.02, respectively (n = 3). It is interesting that by the shake-flask method, the log D value of [^{99m}Tc]**25** containing an amide group is much higher than that of [^{99m}Tc]**23** containing a carbonyl group. However, the reverse-phase HPLC retention times for **10a** and **16** were 9.90 and 8.47 min (coinjection HPLC profiles are shown in the Supporting Information), respectively, indicating that the replacement of the carbonyl group with an amide group decreased the lipophilicity of the complex.

Biodistribution Studies in Mice and Blocking Studies. Because **10a** and **10b** possess low nanomolar affinity for σ_1 receptors, the kinetics of the corresponding [^{99m}Tc]**23** and [^{99m}Tc]**24** complexes were investigated in vivo by biodistribution studies in male ICR mice. The respective data obtained at 2, 15, 30, 60, 120, and 240 min postinjection in various organs of interest are shown in Tables 2 and 3. [^{99m}Tc]**23** displayed high initial brain uptake (2.94 ± 0.41% injected dose (ID)/g at 2 min postinjection) with rather slow clearance (1.52 ± 0.17% ID/g at 60 min postinjection) and relatively high brain-to-blood ratios (3.03, 2.92, and 3.28 at 30, 60, and 240 min postinjection, respectively). The accumulation of [^{99m}Tc]**23** in the brain peaked at 15 min postinjection with 3.25 ± 0.38% ID/g. The lungs showed significantly high uptake at 2 min postinjection (35.08 ± 8.01% ID/g), which considerably decreased thereafter reaching 6.77 ± 0.91% ID/g at 30 min postinjection. The radiotracer accumulation in the thyroid was very low at 240 min postinjection, indicating that no pertechnetate was formed in vivo.

[^{99m}Tc]**24** also displayed high initial brain uptake (2.13 ± 0.24% ID/g at 2 min postinjection). The blood clearance rate of [^{99m}Tc]**24** was faster than that of [^{99m}Tc]**23**, resulting in higher brain-to-blood ratios (3.56, 4.37, 4.15, and 4.35 at 30, 60, 120, and 240 min postinjection, respectively). High initial

Table 2. Biodistribution of [^{99m}Tc]23 in Male ICR Mice[a]

organ	2 min	15 min	30 min	60 min	120 min	240 min
blood	1.88 ± 0.30	0.99 ± 0.14	0.74 ± 0.02	0.52 ± 0.08	0.52 ± 0.07	0.32 ± 0.04
brain	2.94 ± 0.41	3.25 ± 0.38	2.24 ± 0.35	1.52 ± 0.17	1.30 ± 0.24	1.05 ± 0.16
heart	10.20 ± 1.40	3.93 ± 0.62	2.81 ± 0.55	1.87 ± 0.31	1.79 ± 0.32	1.31 ± 0.21
liver	10.00 ± 1.25	17.95 ± 2.25	21.00 ± 1.22	19.33 ± 1.67	22.30 ± 1.19	20.31 ± 2.90
spleen	5.03 ± 0.45	6.41 ± 0.99	4.95 ± 0.46	3.20 ± 0.50	2.24 ± 0.22	1.52 ± 0.30
lung	35.08 ± 8.01	9.58 ± 2.60	6.77 ± 0.91	4.88 ± 1.36	4.30 ± 0.86	3.44 ± 0.83
kidney	19.27 ± 2.08	16.99 ± 1.95	16.40 ± 1.36	13.88 ± 1.28	15.05 ± 1.33	12.94 ± 1.35
small intestine[b]	5.54 ± 0.83	10.52 ± 1.92	12.52 ± 1.58	13.35 ± 1.37	16.59 ± 2.00	9.75 ± 1.24
stomach[b]	1.73 ± 0.22	2.89 ± 0.37	2.47 ± 0.44	2.64 ± 0.22	2.08 ± 0.48	1.51 ± 0.25
muscle	2.94 ± 0.76	3.06 ± 1.50	1.55 ± 0.26	1.12 ± 0.41	0.81 ± 0.08	0.61 ± 0.13
thyroid[b]	0.26 ± 0.04	0.24 ± 0.14	0.25 ± 0.04	0.14 ± 0.04	0.16 ± 0.03	0.15 ± 0.04
brain/blood	1.56	3.28	3.03	2.92	2.50	3.28

[a]Data are expressed as percentage of injected dose per gram, mean ± SD, n = 5. [b]Percentage of injected dose per organ.

dx.doi.org/10.1021/jm5009488 | J. Med. Chem. XXXX, XXX, XXX–XXX

Table 3. Biodistribution of [^{99m}Tc]24 in Male ICR Mice[a]

organ	2 min	15 min	30 min	60 min	120 min	240 min
blood	2.69 ± 0.35	0.95 ± 0.20	0.52 ± 0.02	0.35 ± 0.03	0.27 ± 0.02	0.23 ± 0.05
brain	2.13 ± 0.24	2.03 ± 0.22	1.85 ± 0.18	1.53 ± 0.13	1.12 ± 0.21	1.00 ± 0.19
heart	12.51 ± 1.27	5.04 ± 0.97	3.91 ± 0.39	2.53 ± 0.25	1.44 ± 0.22	1.55 ± 0.27
liver	10.85 ± 1.78	18.76 ± 3.69	21.71 ± 2.10	21.73 ± 2.49	20.90 ± 2.06	21.83 ± 3.58
spleen	5.86 ± 2.25	10.34 ± 1.82	10.97 ± 1.57	9.44 ± 0.92	6.44 ± 0.69	6.37 ± 0.54
lung	45.40 ± 6.66	17.51 ± 3.55	11.31 ± 1.92	8.62 ± 1.01	5.61 ± 1.34	4.88 ± 0.91
kidney	19.58 ± 1.85	18.23 ± 1.51	17.26 ± 1.75	13.91 ± 1.39	11.43 ± 0.95	10.99 ± 1.31
small intestine[b]	3.79 ± 0.79	8.42 ± 3.62	16.49 ± 0.84	11.21 ± 2.99	14.30 ± 4.07	12.17 ± 6.38
stomach[b]	1.10 ± 0.10	2.01 ± 0.11	3.04 ± 0.67	1.99 ± 0.25	1.56 ± 0.11	2.36 ± 0.79
muscle	4.69 ± 0.81	2.30 ± 0.16	2.01 ± 0.21	1.39 ± 0.15	1.06 ± 0.31	0.77 ± 0.09
thyroid[b]	0.10 ± 0.03	0.10 ± 0.01	0.08 ± 0.01	0.07 ± 0.01	0.07 ± 0.01	0.09 ± 0.01
brain/blood	0.79	2.14	3.56	4.37	4.15	4.35

[a]Data are expressed as percentage of injected dose per gram, mean ± SD, n = 5. [b]Percentage of injected dose per organ.

Table 4. Effects of Preinjection of Haloperidol (0.1 mL, 1.0 mg/kg) 5 min Prior to Radiotracer Injection on the Biodistribution of [^{99m}Tc]23 in Male ICR Mice[a]

organ	60 min (control)	60 min (blocking)	% blocking	p^c	120 min (control)	120 min (blocking)	% blocking	p^c
blood	0.52 ± 0.08	0.55 ± 0.03	6	0.444	0.52 ± 0.07	0.52 ± 0.05	0	0.942
brain	1.52 ± 0.17	0.82 ± 0.08	−46	<0.001	1.30 ± 0.24	0.80 ± 0.17	−38	0.005
heart	1.87 ± 0.31	1.50 ± 0.27	−20	0.076	1.79 ± 0.32	1.26 ± 0.23	−30	0.017
liver	19.33 ± 1.67	21.04 ± 3.65	9	0.366	22.30 ± 1.19	23.73 ± 2.44	6	0.271
spleen	3.20 ± 0.50	1.74 ± 0.28	−46	<0.001	2.24 ± 0.22	1.26 ± 0.33	−44	<0.001
lung	4.88 ± 1.36	4.01 ± 0.90	−18	0.268	4.30 ± 0.86	3.39 ± 0.92	−21	0.144
kidney	13.88 ± 1.28	13.73 ± 1.20	−1	0.855	15.05 ± 1.33	14.60 ± 2.29	−3	0.714
small intestine[b]	13.35 ± 1.37	18.38 ± 2.02	38	0.002	16.59 ± 2.00	16.29 ± 3.02	−2	0.859
stomach[b]	2.64 ± 0.22	4.49 ± 0.69	70	<0.001	2.08 ± 0.48	2.75 ± 1.00	32	0.211
muscle	1.12 ± 0.41	0.54 ± 0.07	−52	0.015	0.81 ± 0.08	0.34 ± 0.28	−58	0.007
thyroid[b]	0.14 ± 0.04	0.14 ± 0.03	0	0.931	0.16 ± 0.03	0.16 ± 0.04	0	0.991

[a]Data are expressed as percentage of injected dose per gram, mean ± SD, n = 5. [b]Percentage of injected dose per organ. [c]p values for the control versus blocking group at 60 and 120 min postinjection calculated by Student's t test (independent, two-tailed).

uptake and fast clearance from the lungs were also observed for [^{99m}Tc]**24** (45.40 ± 6.66 and 11.31 ± 1.92% ID/g at 2 and 30 min postinjection, respectively). The radiotracer accumulation in the thyroid was very low at 240 min postinjection, indicating that no pertechnetate was formed in vivo.

To detect specific binding of [^{99m}Tc]**23** in vivo, blocking studies using haloperidol as the blocking agent were conducted. Haloperidol (1.0 mg/kg) was injected 5 min prior to the radiotracer injection. The blocking results at 60 and 120 min postinjection are shown in Table 4. A significant reduction of the radiotracer accumulation was observed in the brain (46% and 39% at 60 and 120 min postinjection, respectively). Moreover, radiotracer accumulation in the spleen, which is known to possess high levels of σ_1 receptors, was significantly reduced by 46% ($p < 0.001$). These results demonstrated the specific binding of [^{99m}Tc]**23** to σ_1 receptors in vivo. The results obtained from the blocking studies with [^{99m}Tc]**24** at 60 min postinjection are shown in Table 5. As radiotracer accumulation in the brain was also significantly reduced (43%, $p < 0.001$) by haloperidol pretreatment, the specific binding of [^{99m}Tc]**24** to σ_1 receptors in the brain was suggested.

*In Vivo Stability of [^{99m}Tc]**23***. The metabolism of [^{99m}Tc]**23** was investigated in brain, plasma, and liver samples from male ICR mice at 15 min postinjection (33 MBq, 0.15 mL). The HPLC chromatograms of [^{99m}Tc]**23** are shown in Figure 3. In the liver extract, 63% of the total radioactivity corresponded to [^{99m}Tc]**23**. Less lipophilic metabolites M5, M1, M2, M3, M4, and M6 were detected at retention times of 2.36, 3.78, 4.60, 6.30, 7.59, and 8.96 min, respectively. In plasma samples, the parent radiotracer [^{99m}Tc]**23** accounted for 48% of the total activity. Two less lipophilic metabolites, M1 (39%) and M2 (13%), were detected at retention times of 3.83 and 4.49 min, respectively. In brain samples, the parent compound [^{99m}Tc]**23** accounted for 94% of the total activity, and only small amounts

Table 5. Effects of Preinjection of Haloperidol (0.1 mL, 1.0 mg/kg) 5 min Prior to Radiotracer Injection on the Biodistribution of [^{99m}Tc]24 in Male ICR Mice[a]

organ	60 min (control)	60 min (blocking)	% blocking	p^c
blood	0.35 ± 0.03	0.39 ± 0.03	11	0.034
brain	1.53 ± 0.13	0.87 ± 0.08	−43	<0.001
heart	2.53 ± 0.25	2.14 ± 0.31	−15	0.060
liver	21.73 ± 2.49	22.52 ± 2.25	4	0.614
spleen	9.44 ± 0.92	10.45 ± 2.14	11	0.361
lung	8.62 ± 1.01	8.94 ± 1.50	4	0.698
kidney	13.91 ± 1.39	13.21 ± 1.70	−5	0.493
small intestine[b]	11.21 ± 2.99	13.85 ± 5.08	24	0.346
stomach[b]	1.99 ± 0.25	3.65 ± 0.71	83	0.003
muscle	1.39 ± 0.15	1.43 ± 0.24	3	0.738
thyroid[b]	0.07 ± 0.01	0.10 ± 0.01	43	0.022

[a]Data are expressed as percentage of injected dose per gram, mean ± SD, n = 5. [b]Percentage of injected dose per organ. [c]p values for the control versus blocking group at 60 min postinjection calculated by Student's t test (independent, two-tailed).

dx.doi.org/10.1021/jm5009488 | J. Med. Chem. XXXX, XXX, XXX−XXX

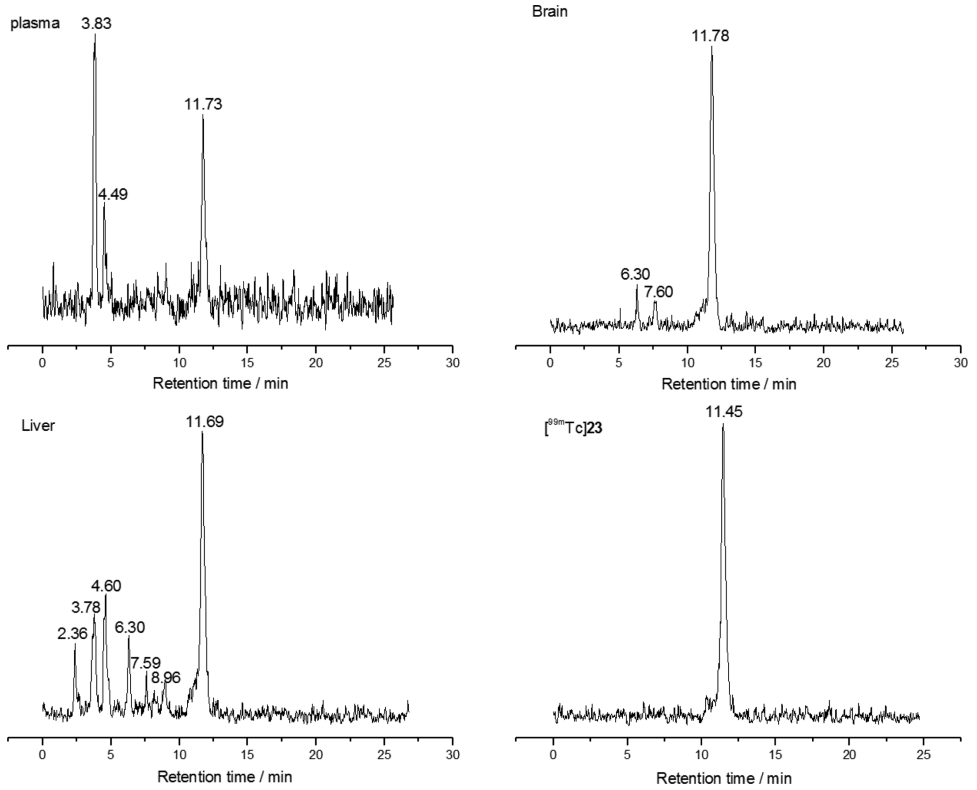

Figure 3. Analytical HPLC chromatograms of radioactive compounds in mouse plasma, brain, and liver samples at 15 min after intravenous injection of [^{99m}Tc]**23** (33 MBq, 0.15 mL).

of two less lipophilic radiometabolites were detected at retention times of 6.30 min (M3, 2% of total activity) and 7.60 min (M4, 4% of total activity), respectively. It is interesting that the small amount of the two less lipophilic radiometabolites detected in the brain are different from those in plasma samples, suggesting that radiometabolites in the blood do not enter the brain.

*Effect of P-gp on the Brain Uptake of [^{99m}Tc]**23** in Mice.* It is well-known that the blood–brain barrier expresses high levels of permeability-glycoprotein (P-gp). The function of P-gp is inversely related to the brain uptake of its substrate.[40] To identify whether [^{99m}Tc]**23** is a substrate for P-gp at the blood–brain barrier in vivo, biodistribution studies with cyclosporine A, an inhibitor of P-gp, were performed. The results are shown in Figure 4. Administration of cyclosporine A 60 min prior to [^{99m}Tc]**23** injection considerably increased the initial brain uptake of the radiotracer from 2.71 ± 0.60 to 4.40 ± 0.61% ID/g at 2 min postinjection. The blood accumulation of the radiotracer remained at almost the same level (saline, 1.71 ± 0.24% ID/g; cyclosporine A, 1.90 ± 0.21% ID/g at 2 min postinjection). These data suggested that [^{99m}Tc]**23** may be a substrate for P-gp.

*Uptake of [^{99m}Tc]**23** in C6 and DU145 Tumor Cell Lines.* In recent years, different levels of σ_1 receptor expression were found in various tumor cell lines.[13−15] For further characterization of the potential applications of [^{99m}Tc]**23** for imaging σ_1 receptors in tumors, in vitro cell uptake studies were performed in C6 and DU145 cell lines according to the methods reported in the literature.[28]

The uptake of [^{99m}Tc]**23** in C6 glioma cells is shown in Figure 5. An increase in the radiotracer uptake was observed with longer incubation time. The percentage uptake was 2.98, 3.83, and 4.05% after incubation at room temperature for 15, 30, and 60 min, respectively. Blocking studies were conducted with haloperidol, DTG, and SA4503 as blocking agents. The blocking effects on [^{99m}Tc]**23** uptake in C6 glioma cells are

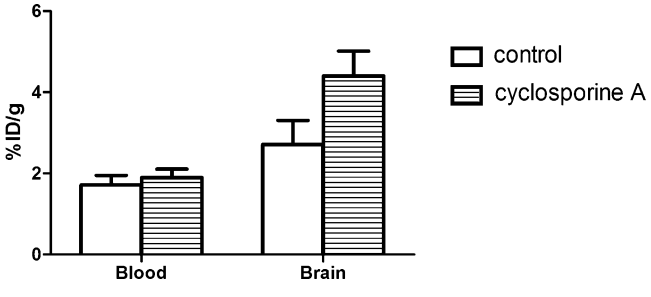

Figure 4. Effect of P-gp on brain uptake of [^{99m}Tc]**23** in mice. Student's *t* test (independent, two-tailed) was performed, $p < 0.01$ for brain.

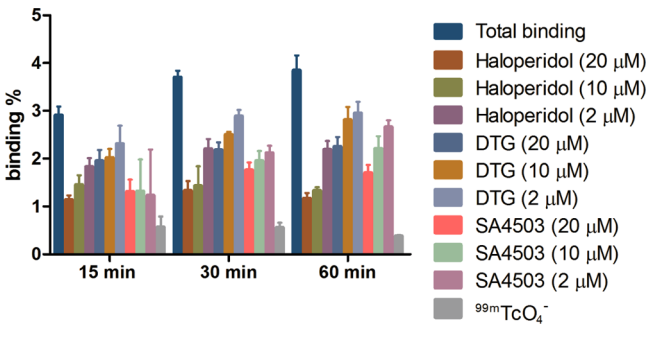

Figure 5. In vitro uptake of [^{99m}Tc]**23** in C6 glioma cells.

dx.doi.org/10.1021/jm5009488 | J. Med. Chem. XXXX, XXX, XXX−XXX

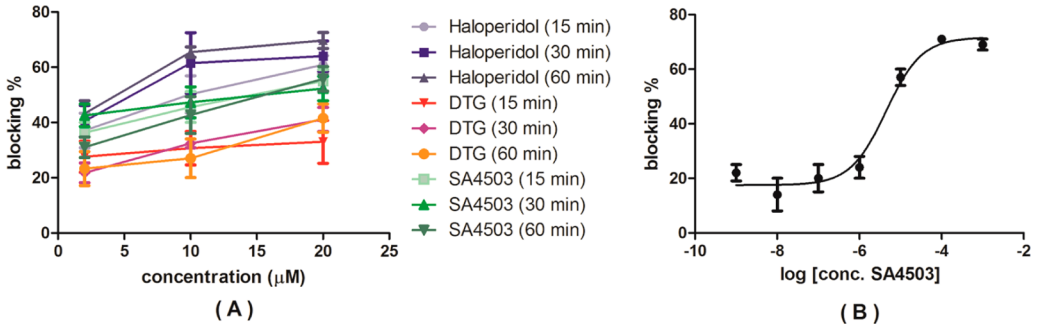

Figure 6. In vitro blocking results of [^{99m}Tc]**23** in tumor cells. (A) [^{99m}Tc]**23** in C6 glioma cells with various inhibitors at different incubation times. (B) [^{99m}Tc]**23** in DU145 prostate cancer cells with different concentrations of SA4503 at 60 min.

Table 6. Effects of Preinjection of Haloperidol (1.0 mg/kg) or DTG (3 μmol/kg) 5 min Prior to Radiotracer Injection on the Biodistribution of [^{99m}Tc]23 in C6 Glioma-Bearing Mice[a]

organ	control	haloperidol	% blocking[c]	p[d]	control	DTG	% blocking[c]	p[d]
blood	0.34 ± 0.04	0.37 ± 0.02	10	0.158	0.34 ± 0.04	0.29 ± 0.07	−14	0.227
brain	1.37 ± 0.11	0.68 ± 0.13	−50	<0.001	1.37 ± 0.11	0.96 ± 0.26	−30	0.015
heart	1.90 ± 0.30	1.00 ± 0.04	−47	<0.001	1.90 ± 0.30	0.93 ± 0.20	−51	<0.001
liver	14.09 ± 1.25	15.21 ± 1.90	8	0.320	14.09 ± 1.25	13.15 ± 2.36	−7	0.465
spleen	3.82 ± 0.46	2.02 ± 0.06	−47	<0.001	3.82 ± 0.46	2.18 ± 0.92	−43	0.010
lung	5.32 ± 1.67	3.22 ± 0.75	−40	0.054	5.32 ± 1.67	3.23 ± 1.04	−39	0.066
kidney	15.86 ± 0.49	15.80 ± 3.01	0	0.967	15.86 ± 0.49	13.15 ± 1.64	−17	0.009
small intestine[b]	16.66 ± 2.20	17.66 ± 2.41	6	0.539	16.66 ± 2.20	17.57 ± 5.15	5	0.732
stomach	3.70 ± 1.00	4.21 ± 0.73	14	0.423	3.70 ± 1.00	2.59 ± 0.55	−30	0.088
muscle	0.63 ± 0.13	0.38 ± 0.06	−39	0.009	0.63 ± 0.13	0.35 ± 0.09	−44	0.008
tumor	2.18 ± 0.37	1.16 ± 0.10	−47	0.001	2.18 ± 0.37	1.33 ± 0.10	−39	0.003
tumor/muscle	3.47	3.05			3.47	3.77		
tumor/blood	6.39	3.10			6.39	4.55		

[a]Data are expressed as percentage of injected dose per gram, mean ± SD, n = 5. [b]Percentage of injected dose per organ. [c]%blocking = (blocking−control)/control ×100%. [d]p values for the control versus blocking group at 60 min postinjection calculated by Student's t test (independent, two-tailed).

time- and dose-dependent (Figure 6A). After a 60 min coincubation with 2, 10, and 20 μM haloperidol, the uptake was significantly reduced by 43%, 65%, and 69%, respectively. A similar, strong reduction of cell uptake was found by treatment with SA4503 at the same doses (31%, 42%, and 54% inhibition), but the effects were considerably milder with DTG (24−41% inhibition) due to the moderate affinity of DTG for σ_1 receptors. Among these blocking agents, SA4503 showed high affinity and selectivity for σ_1 receptors. Thus, blocking studies of [^{99m}Tc]**23** in DU145 prostate cells were performed with SA4503 as the blocking agent at 60 min. Furthermore, a dose-dependent blocking effect of SA4503 on [^{99m}Tc]**23** uptake in DU145 prostate cancer cells was shown (Figure 6B). These data demonstrated that [^{99m}Tc]**23** binds specifically to σ_1 receptors in C6 glioma cells and DU145 prostate cancer cells.

Blocking Studies in C6 Glioma-Bearing Mice. To investigate the specific binding in tumors in vivo, blocking studies of [^{99m}Tc]**23** biodistribution in C6 glioma-bearing mice were performed using haloperidol (1.0 mg/kg) and DTG (3 μmol/kg) as blocking agents. The blocking results are shown in Table 6. Administration of haloperidol and DTG significantly decreased the accumulation of [^{99m}Tc]**23** in the tumors by 47% and 39%, respectively, at 60 min, suggesting the specific binding of [^{99m}Tc]**23** to σ_1 receptors in solid tumors. Similar to what was found for biodistribution in normal mice, brain uptake was also decreased by 50% with haloperidol and by 30% with DTG, reflecting different affinities of these inhibitors for σ_1 receptors. A strong reduction of radiotracer accumulation was observed in organs known to contain σ_1 receptors, such as the heart, spleen, and lung; this result is in good agreement with the results of blocking studies in normal mice.

DISCUSSION

The σ_1 receptor belongs to a unique family of proteins related to a number of CNS diseases.[4,5,11] PET or SPECT neuroimaging with radiotracers possessing appropriate affinity and high specificity for σ_1 receptors provides an important tool to investigate the pathophysiology of CNS diseases.[9,41] There are some candidates, such as [^{11}C]SA4503, that are available as PET imaging agents for σ_1 receptors. However, few ^{99m}Tc-labeled radiotracers are suitable as SPECT imaging agents for σ_1 receptors. Formidable challenges, such as low brain uptake, hinder the development of ^{99m}Tc-based CNS receptor imaging agents. In our previous work, we found that 1-(1,3-benzodioxol-5-ylmethyl)-4-(4-bromobenzyl)piperazine (BP-Br) and its analogues, such as 1-(1,3-benzodioxol-5-ylmethyl)-4-(4-iodobenzyl)piperazine (BP-I), possessed subnanomolar affinity and high subtype selectivity for σ_1 receptors.[42] Later, a 2-fluoroethoxy group was introduced at the *para*-position of the benzyl moiety resulting in compound **7**, which retained nanomolar affinity and showed even higher subtype selectivity for σ_1 receptors. Moreover, the radioligand [^{18}F]**7** exhibited high initial brain uptake and specific binding to σ_1 receptors in vivo.[31] Recently, we reported a simpler method for synthesizing

dx.doi.org/10.1021/jm5009488 | J. Med. Chem. XXXX, XXX, XXX−XXX

[(Cp-R)M(CO)$_3$] (M = ^{99m}Tc, Re) complexes under milder reaction conditions and with higher yield compared to the widely reported DLT reaction.[28] The ^{99m}Tc-labeled selective σ_2 receptor radioligand developed in our recent work showed relatively high initial brain uptake and specific binding to the σ receptors in brain tumors.[28] These results encouraged us to concentrate on the further exploration of ^{99m}Tc-labeled probes for σ_1 receptor imaging in vivo. In this current study, we used [^{18}F]**7** as the lead compound to develop ^{99m}Tc-labeled radiotracers for the SPECT imaging of the σ_1 receptors using an integrated approach. Because the linker may significantly affect receptor binding and brain uptake, we replaced the benzyl moiety carrying a [(Cp-R)M(CO)$_3$] unit with an electron-withdrawing group and connected the [(Cp-R)M(CO)$_3$] unit to a 1-piperonylpiperazine moiety via different carbon chain lengths. The designed complexes still possess two basic nitrogen atoms flanked by two hydrophobic regions in accordance with the pharmacophore model proposed by Glennon.[32]

To meet the first and possibly the most easily achieved criterion, the rhenium surrogates were synthesized to examine whether the complexes containing the [(Cp-R)M(CO)$_3$] unit retained binding affinity for σ_1 receptors. In vitro binding assays showed that compounds **10a** and **10b** exhibited comparable low nanomolar affinity and comparable or improved subtype selectivity for σ_1 receptors relative to SA4503. Although several rhenium complexes were developed as σ_1 receptor ligands in the past decades, few showed nanomolar affinities.[24−29] The retained high affinity and subtype selectivity of **10a** and **10b** for σ_1 receptors showed that the integrated strategy of assembling the molecular structure of σ_1 receptor ligands reported in this paper was successful. Moreover, **10a** displayed low affinity for VAChT and thus high σ_1/VAChT selectivity.

To find radiotracers with suitable kinetic profiles, we prepared the corresponding ^{99m}Tc-labeled complexes [^{99m}Tc]**23** and [^{99m}Tc]**24** of surrogates **10a** and **10b** for in vitro and in vivo studies. Among the in vitro properties, suitable lipophilicity is important for adequate blood−brain barrier permeability. The log *D* values of [^{99m}Tc]**23** and [^{99m}Tc]**24** were within the optimal range (2−3) for high brain uptake.[43] In addition, [^{99m}Tc]**23** and [^{99m}Tc]**24** displayed high in vitro stability at room temperature in saline.

Encouraged by the in vitro properties, we performed in vivo biological experiments to evaluate the ^{99m}Tc-labeled complexes as potential SPECT radiotracers. In biodistribution studies in male mice, both [^{99m}Tc]**23** and [^{99m}Tc]**24** exhibited high initial brain uptakes with 2.94 and 2.13% ID/g at 2 min postinjection, respectively. Particularly for [^{99m}Tc]**23**, the radiotracer accumulation in the brain peaked at 15 min postinjection with 3.25% ID/g, which is higher than any of the previously reported ^{99m}Tc-labeled complexes for σ_1 receptor imaging.[24] Over the past decades, considerable interest has been given to the development of CNS receptor-based ^{99m}Tc probes due to the ideal nuclear physical characteristics for routine nuclear medicine diagnostics and ready availability of ^{99m}Tc. Because technetium is a transition metal, a fundamental challenge exists in the pharmacologically acceptable integration of the technetium chelate unit into CNS receptor ligands. The successful development of [2-[[2-[[[3-(4-chlorophenyl)-8-methyl-8-azabicyclo[3.2.1]oct-2-yl]methyl](2-mercaptoethyl)-amino]ethyl]amino]ethanethiolato-(3-)-*N*2,*N*2′,*S*2,*S*2′]oxo-[1R-(*exo-exo*)]-[^{99m}Tc]technetium ([^{99m}Tc]TRODAT-1) for imaging dopamine transporters in the brain brought optimism to the investigation of ^{99m}Tc-based CNS receptor ligands. However, [^{99m}Tc]TRODAT-1 is the only ^{99m}Tc-based CNS receptor radiotracer used in clinic, and it still suffers from relatively low brain uptake.[44] The low brain uptake remains the bottleneck in the development of ^{99m}Tc-based CNS receptor radiotracers, leading to decreasing interest in this laborious field. The high accumulation of [^{99m}Tc]**23** in the brain, together with the nanomolar affinity for σ_1 receptors, brightens the future for ^{99m}Tc-based CNS receptor radiotracers.

To measure the specific binding of radiotracers to σ_1 receptors in vivo, we used haloperidol, the most widely used σ_1 antagonist, as a blocking agent to perform the blocking studies in vivo. Pretreatment of mice with haloperidol (1.0 mg/kg) significantly reduced the accumulation of radiotracer in the brain (46% and 43% reduction for [^{99m}Tc]**23** and for [^{99m}Tc]**24**, respectively, at 60 min postinjection). Although the percentages of inhibition were lower than that of [^{18}F]**7** (71% reduction at 60 min postinjection), these data still suggested that the accumulation of [^{99m}Tc]**23** and [^{99m}Tc]**24** could represent specific binding to σ_1 receptors in vivo.

For the development of a brain radiotracer, it is very important to investigate the metabolic profile of radioligands in vivo. If radiometabolites could enter the brain, the binding signals in the brain would be influenced. Therefore, the in vivo metabolism of [^{99m}Tc]**23** in the mouse brain, plasma, and liver samples was studied. The results obtained at 15 min postinjection showed that the parent compound [^{99m}Tc]**23** was the main radioactive species present in the mouse brain (94%). The two radiometabolites in the blood were different from those in the brain, indicating no entry of radioactive metabolites into the brain through blood.

Because of the high expression of P-gp at the blood−brain barrier, the identification of a brain radiotracer as a substrate of P-gp is currently an important issue.[45] To further investigate the identification of [^{99m}Tc]**23** as a substrate of P-gp in vivo, we performed biodistribution studies at 2 min postinjection of the radiotracer using cyclosporine A as a blocking agent. P-gp inhibition by cyclosporine A increased the brain uptake of [^{99m}Tc]**23** approximately 1.6-fold without changing the radiotracer concentration in the blood, indicating that [^{99m}Tc]**23** is likely a substrate of P-gp. Thus, the effects of P-gp on the brain uptake need to be considered for the evaluation of CNS receptor-based radiotracers.

In addition to the high density of σ_1 receptors in the CNS, high expression was also observed in many human tumor cell lines.[12,13,16,46] For example, the maximum specific binding (B_{max}) values of σ_1 receptors in C6 glioma cell lines and in prostate tumor cell lines from rats are approximately 980 and 1800 fmol/mg protein using radioligand (+)-[^{3}H]-pentazocine, respectively.[13,46] Considering the relatively higher affinity for σ_1 receptors and higher σ_1/VAChT selectivity, [^{99m}Tc]**23** was selected for the evaluation of potential applications in tumor imaging.

Haloperidol is generally accepted as a σ_1 antagonist with high affinity for σ receptors ($K_i(\sigma_1)$ = 4.95 nM, $K_i(\sigma_2)$ = 20.7 nM)[31] and moderate to high affinity for dopamine D$_2$, adrenergic, and serotonin receptors.[47] DTG has moderate affinity for σ receptors and low affinities for other receptors. SA4503 is a selective ligand with nanomolar affinity for σ_1 receptors and low or negligible affinity for 36 other receptors, ion channels and components of second messenger systems.[48] To investigate the specific binding of [^{99m}Tc]**23** to σ_1 receptors in tumors, we first performed cell uptake studies in C6 glioma cells by pretreat-

dx.doi.org/10.1021/jm5009488 | J. Med. Chem. XXXX, XXX, XXX−XXX

ment with various concentrations of haloperidol, DTG, and SA4503. The radiotracer uptake in C6 glioma cell lines was significantly reduced in a time- and dose-dependent manner. In addition, a higher affinity of competitors for σ receptors was correlated with a stronger reduction of radiotracer accumulation. Blocking studies of [^{99m}Tc]**23** in DU145 prostate cancer cells also displayed a reduction of radiotracer uptake in a dose-dependent manner. These results demonstrated the specific binding of [^{99m}Tc]**23** to σ_1 receptors in tumor cell lines. To further determine the specific binding in solid tumors in vivo, blocking studies in C6 glioma-bearing mice were performed. Pretreatment with haloperidol or DTG resulted in 47% or 39% reduction of radiotracer accumulation in tumors at 60 min postinjection, respectively, reflecting specific binding of [^{99m}Tc]**23** to σ_1 receptors in C6 glioma tumors.

CONCLUSION

In conclusion, the novel radiotracer [^{99m}Tc]**23** possesses advantageous characteristics such as nanomolar affinity for σ_1 receptors, high brain uptake, and specific binding to σ_1 receptors in the normal brain, tumor cell lines, and C6 glioma tumors. This ^{99m}Tc-labeled probe warrants further evaluation as a potential SPECT radiotracer for the investigation of σ_1 receptor density in the CNS and as a putative imaging agent for σ_1 receptor expression in brain tumors. The encouraging results obtained in this paper also indicate a advance in the development of CNS receptor-based ^{99m}Tc-labeled probes. Suitable ^{99m}Tc-based CNS receptor imaging agents may be attainable if the [(Cp-R)M(CO)$_3$] unit can be incorporated into selective receptor ligands via an appropriate linker using the integrated approach. Developments of new ^{99m}Tc-labeled radiotracers with improved brain uptake and high specific binding to σ_1 receptors in vivo are in progress.

EXPERIMENTAL SECTION

General Information. The reagents and chemicals, thin layer chromatography (TLC), ^{1}H NMR spectra, ^{13}C NMR spectra, mass spectrometry (MS), HPLC, and mice were obtained and handled very similarly to previous work.[31] These details are provided in the Supporting Information. The HPLC method was used to determine the purity of target compounds. All the final compounds were tested with purity of more than 95% (HPLC profiles are shown in the Supporting Information).

^{99m}Tc-pertechnetate was eluted from a commercial ^{99}Mo−^{99m}Tc generator obtained from Beijing Atomic High-Tech Co. Samples were analyzed and separated on an Agela Venusil MP C18 column (250 mm × 4.6 mm, 5 μm) using acetonitrile with 0.1% trifluoroacetic acid (TFA) and water with 0.1% TFA as the mobile phase at a flow rate of 1 mL/min.

All procedures related to animal experiments were performed in compliance with relevant laws and institutional guidelines. All of the animal experiments were approved by the Institutional Animal Care and Use Committee of Beijing Normal University.

Chemistry. *(4-Bromobutylcarbonyl)cyclopentadienyl Tricarbonyl Rhenium (**8b**).* Under N_2, cyclopentadienyl tricarbonyl rhenium (153.8 mg, 0.46 mmol) was added to a solution of 5-bromovaleryl chloride (182.0 mg, 0.91 mmol) in dried CH_2Cl_2 (5 mL). The solution was cooled to 0 °C, followed by the slow addition of dried aluminum chloride (71.7 mg, 0.54 mmol). The mixture was warmed to room temperature, stirred for 4 h, and poured over ice−H_2O and 4 mL $NH_3\cdot H_2O$. The crude product was extracted with CH_2Cl_2, dried with anhydrous $MgSO_4$, and purified by silica gel column chromatography (ethyl acetate/petroleum ether = 1/10, v/v) to afford **8b** as a white oil (172.6 mg, 75%). ^{1}H NMR (400 MHz, $CDCl_3$) δ 5.99 (t, J = 2.3 Hz, 2H), 5.41 (t, J = 2.3 Hz, 2H), 3.44 (t, J = 6.3 Hz, 2H), 2.64 (t, J = 6.8 Hz, 2H), 1.95−1.81 (m, 4H). ESI-MS, [M + H]$^+$ (m/z = 498.7).

*(5-Bromopentylcarbonyl)cyclopentadienyl Tricarbonyl Rhenium (**8c**).* The procedure described for the synthesis of **8b** was applied to 6-bromohexanoyl chloride to afford **8c** as a white solid (87%); mp 76.5−78.5 °C. ^{1}H NMR (400 MHz, $CDCl_3$) δ 5.98 (t, J = 2.2 Hz, 2H), 5.40 (t, J = 2.2 Hz, 2H), 3.42 (t, J = 6.7 Hz, 2H), 2.61 (t, J = 7.2 Hz, 2H), 1.93−1.86 (m, 2H), 1.76−1.68 (m, 2H), 1.51−1.45 (m, 2H). ESI-MS, [M + H]$^+$ (m/z = 512.9).

*3-(4-(1,3-Benzodioxol-5-ylmethyl)piperazin-1-yl)-propylcarbonylcyclopentadienyl Tricarbonyl Rhenium (**10a**).* To a solution of **8a** (55.0 mg, 0.11 mmol) in 3 mL of toluene and 3 mL of triethylamine, 1-piperonylpiperazine (**9**, 28.4 mg, 0.13 mmol) and KI (9.1 mg, 0.05 mmol) were added successively. The mixture was heated to 115 °C and stirred in the dark for 4 h. After cooling to room temperature, the reaction mixture was concentrated under vacuum. Purification by silica gel column chromatography (ethyl acetate/petroleum ether/triethylamine = 1/10/1, v/v/v) afforded **10a** as an orange oil (11.2 mg, 16%). ^{1}H NMR (400 MHz, $CDCl_3$) δ 6.83 (s, 1H), 6.73 (s, 2H), 5.97 (t, J = 2.1 Hz, 2H), 5.93 (s, 2H), 5.38 (t, J = 2.1 Hz, 2H), 3.39 (s, 2H), 2.60 (t, J = 6.9 Hz, 2H), 2.42−2.33 (m, 10H), 1.90−1.83 (m, 2H). ^{13}C NMR (100 MHz, $CDCl_3$) δ 194.69, 191.91, 147.58, 146.56, 131.91, 122.25, 109.54, 107.82, 100.84, 96.62, 87.73, 85.05, 62.69, 57.31, 52.96, 52.69, 36.56, 21.60. TOF-ES$^+$-MS, [M + H]$^+$: m/z calcd for $C_{24}H_{26}N_2O_6{}^{185}$Re 623.1321; found 623.1317.

*4-(4-(1,3-Benzodioxol-5-ylmethyl)piperazin-1-yl)-butylcarbonylcyclopentadienyl Tricarbonyl Rhenium (**10b**).* The procedure described for the synthesis of **10a** was applied to **8b** to afford **10b** as an orange oil (22%). ^{1}H NMR (400 MHz, $CDCl_3$) δ 6.85 (s, 1H), 6.74 (d, J = 0.8 Hz, 2H), 6.00 (t, J = 2.3 Hz, 2H), 5.93 (s, 2H), 5.38 (t, J = 2.3 Hz, 2H), 3.41 (s, 2H), 2.61 (t, J = 7.3 Hz, 2H), 2.57−2.45 (m, 8H), 2.35 (t, J = 7.5 Hz, 2H), 1.74−1.66 (m, 2H), 1.56−1.48 (m, 2H). ^{13}C NMR (100 MHz, $CDCl_3$) δ 195.02, 191.85, 147.58, 146.53, 132.10, 122.22, 109.53, 107.81, 100.84, 96.12, 87.90, 85.13, 62.77, 57.98, 53.20, 52.95, 38.61, 26.17, 22.41. TOF-ES$^+$-MS, [M + H]$^+$: m/z calcd for $C_{25}H_{28}N_2O_6{}^{185}$Re 637.1477; found 637.1454.

*5-(4-(1,3-Benzodioxol-5-ylmethyl)piperazin-1-yl)-pentylcarbonylcyclopentadienyl Tricarbonyl Rhenium (**10c**).* The procedure described for the synthesis of **10a** was applied to **8c** to afford **10c** as an orange oil (46%). ^{1}H NMR (400 MHz, $CDCl_3$) δ 6.85 (s, 1H), 6.74 (s, 2H), 5.98 (t, J = 2.2 Hz, 2H), 5.94 (s, 2H), 5.40 (t, J = 2.2 Hz, 2H), 3.41 (s, 2H), 2.59 (t, J = 7.3 Hz, 2H), 2.46 (s, 8H), 2.34 (t, J = 7.3 Hz, 2H), 1.73−1.66 (m, 2H), 1.56−1.48 (m, 2H), 1.37−1.29 (m, 2H). ^{13}C NMR (100 MHz, $CDCl_3$) δ 195.05, 191.80, 147.57, 146.52, 132.12, 122.20, 109.51, 107.79, 100.81, 96.20, 87.80, 85.12, 62.76, 58.42, 53.24, 52.93, 38.71, 27.08, 26.65, 24.25. TOF-ES$^+$-MS, [M + H]$^+$: m/z calcd for $C_{26}H_{30}N_2O_6{}^{185}$Re 651.1634; found 651.1633.

*2-(4-(1,3-Benzodioxol-5-ylmethyl)piperazin-1-yl)acetonitrile (**14a**).* To a solution of **9** (204.1 mg, 0.93 mmol) in 6 mL of CH_2Cl_2 and 3 mL of triethylamine, 2-bromoacetonitrile (154.5 mg, 1.29 mmol) was added. The reaction mixture was stirred at room temperature overnight and then poured over water and extracted with CH_2Cl_2. The organic layer was dried with anhydrous $MgSO_4$, filtered, concentrated under vacuum, and purified by silica gel column chromatography using dichloromethane/methanol (100/1, v/v) as the mobile phase to afford **14a** as a light-yellow oil (103.0 mg, 43%). Compared to the method in the literature,[34] the reaction condition is relatively mild, but the yield is relatively low. ^{1}H NMR (400 MHz, $CDCl_3$) δ 6.85 (s, 1H), 6.74 (s, 2H), 5.94 (s, 2H), 3.50 (s, 2H), 3.43 (s, 2H), 2.62 (t, J = 4.7 Hz, 4H), 2.50 (s, 4H). ESI [M + H]$^+$ (m/z = 260.0).

*3-(4-(1,3-Benzodioxol-5-ylmethyl)piperazin-1-yl)propanenitrile (**14b**).* The procedure described for the synthesis of **14a** was applied to 3-bromopropionitrile to afford **14b** as a light-yellow oil (74%). ^{1}H NMR (400 MHz, $CDCl_3$) δ 6.84 (s, 1H), 6.74 (s, 2H), 5.93 (s, 2H), 3.42 (s, 2H), 2.70 (t, J = 7.1 Hz, 2H), 2.51−2.47 (m, 10H). ESI [M + H]$^+$ (m/z = 274.0).

*4-(4-(1,3-Benzodioxol-5-ylmethyl)piperazin-1-yl)butanenitrile (**14c**).* The procedure described for the synthesis of **14a** was applied to 4-bromobutyronitrile to afford **14c** as a light-yellow oil (70%). ^{1}H NMR ($CDCl_3$, 400 MHz) δ 6.85 (s, 1H), 6.74 (d, J = 0.8 Hz, 2H),

dx.doi.org/10.1021/jm5009488 | J. Med. Chem. XXXX, XXX, XXX−XXX

5.93 (s, 2H), 3.42 (s, 2H), 2.47−2.39 (m, 12H), 1.85−1.77 (m, 2H). ESI $[M + H]^+$ (m/z = 288.7).

*2-(4-(1,3-Benzodioxol-5-ylmethyl)piperazin-1-yl)ethanamine (**15a**).* To a solution of $LiAlH_4$ (94.5 mg, 2.49 mmol) in 10 mL of anhydrous diethyl ether, the mixture of **14a** (95.8 mg, 0.37 mmol) in 5 mL of anhydrous tetrahydrofuran (THF) was added dropwise at 0 °C. The reaction mixture was stirred at room temperature overnight. Then, the crude product was poured over ice−H_2O and extracted by ethyl acetate. The organic layer was dried by anhydrous $MgSO_4$, filtered, concentrated under vacuum, and purified by silica gel column chromatography using dichloromethane/methanol/triethylamine (10/1/1, v/v/v) as the mobile phase to afford **15a** as a white solid (31.5 mg, 32%); mp 34.3−35.8 °C. Compared to the method in the literature,[34] the procedure seems more convenient, but the yield is relatively low. ^{1}H NMR (400 MHz, $CDCl_3$) δ 6.85 (s, 1H), 6.74 (d, J = 0.6 Hz, 2H), 5.93 (s, 2H), 3.41 (s, 2H), 2.80 (t, J = 6.2 Hz, 2H), 2.47 (s, 8H), 2.43 (t, J = 6.2 Hz, 2H), 1.91 (s, 2H). ESI $[M + H]^+$ (m/z = 264.1).

*3-(4-(1,3-Benzodioxol-5-ylmethyl)piperazin-1-yl)propan-1-amine (**15b**).* The procedure described for the synthesis of **15a** was applied to **14b** to afford **15b** as a colorless oil (40%). ^{1}H NMR (400 MHz, $CDCl_3$) δ 6.84 (s, 1H), 6.73 (s, 2H), 5.93 (s, 2H), 3.41 (s, 2H), 2.75 (t, J = 6.3 Hz, 2H), 2.47−2.38 (m, 10H), 2.14 (s, 2H), 2.68−1.61 (m, 2H). ESI $[M + H]^+$ (m/z = 278.1).

*4-(4-(1,3-Benzodioxol-5-ylmethyl)piperazin-1-yl)butan-1-amine (**15c**).* The procedure described for the synthesis of **15a** was applied to **14c** to afford **15c** as a colorless oil (45%). ^{1}H NMR (400 MHz, $CDCl_3$) δ 6.85 (s, 1H), 6.74 (d, J = 0.8 Hz, 2H), 5.93 (s, 2H), 3.41 (s, 2H), 2.71 (t, J = 6.7 Hz, 2H), 2.46 (s, 8H), 2.34 (t, J = 7.4 Hz, 2H), 1.80 (s, 2H), 1.56−1.42 (m, 4H). ESI $[M + H]^+$ (m/z = 292.0).

*2-(4-(1,3-Benzodioxol-5-ylmethyl)piperazin-1-yl)-ethylaminocarbonylcyclopentadienyl Tricarbonyl Rhenium (**16a**).* Under N_2, the solution of compound **15a** (25.0 mg, 0.09 mmol) in 1 mL of anhydrous dimethylformamide (DMF) and 30 μL of triethylamine was added to the solution of **13** (38.7 mg, 0.07 mmol) in 1 mL of anhydrous DMF dropwise. The reaction mixture was stirred at room temperature for 4 h. Solvents were removed under vacuum, and the crude product was purified by silica gel column chromatography using ethyl acetate/hexane/triethylamine (10/10/1, v/v/v) as the mobile phase to afford **16a** as a light-orange oil (18.3 mg, 40%). ^{1}H NMR (400 MHz, $CDCl_3$) δ 6.84 (s, 1H), 6.74 (s, 2H), 5.94 (s, 2H), 5.92 (t, J = 2.2 Hz, 2H), 5.36 (t, J = 2.2 Hz, 2H), 3.46−3.41 (m, 4H), 2.59−2.50 (m, 10H). ^{13}C NMR (100 MHz, $CDCl_3$) δ 192.54, 162.22, 147.65, 146.65, 131.83, 122.19, 109.44, 107.86, 100.87, 95.24, 85.96, 84.59, 62.59, 56.07, 52.73, 52.71, 35.86. TOF-ES$^+$-MS, $[M + H]^+$: m/z calcd for $C_{23}H_{25}N_3O_6{}^{185}Re$ 624.1273; found 624.1271.

*3-(4-(1,3-Benzodioxol-5-ylmethyl)piperazin-1-yl)-propylaminocarbonylcyclopentadienyl Tricarbonyl Rhenium (**16b**).* The procedure described for the synthesis of **16a** was applied to **15b** to afford **16b** as a light-orange oil (92%). ^{1}H NMR (400 MHz, $CDCl_3$) δ 7.90 (s, 1H), 6.83 (s, 1H), 6.76 (s, 1H), 6.74 (d, J = 0.9 Hz, 1H), 5.95 (s, 2H), 5.86 (t, J = 2.1 Hz, 2H), 5.34 (t, J = 2.2 Hz, 2H), 3.48 (s, 2H), 3.46−3.42 (m, 2H), 2.56−2.53 (m, 10H), 1.75−1.69 (m, 2H). ^{13}C NMR (100 MHz, $CDCl_3$) δ 192.69, 161.88, 147.62, 146.64, 131.35, 122.33, 109.57, 107.88, 100.90, 96.33, 85.30, 84.73, 62.60, 58.31, 53.47, 52.81, 40.68, 23.85. TOF-ES$^+$-MS, $[M + H]^+$: m/z calcd for $C_{24}H_{27}N_3O_6{}^{185}Re$ 638.1430; found 638.1445.

*4-(4-(1,3-Benzodioxol-5-ylmethyl)piperazin-1-yl)-butylaminocarbonylcyclopentadienyl Tricarbonyl Rhenium (**16c**).* The procedure described for the synthesis of **16a** was applied to **15c** to afford **16c** as a light-orange oil (61%). ^{1}H NMR (400 MHz, $CDCl_3$) δ 6.84 (s, 1H), 6.74 (s, 2H), 6.38 (t, J = 5.2 Hz, 1H), 5.94 (s, 2H), 5.92 (t, J = 2.2 Hz, 2H), 5.35 (t, J = 2.2 Hz, 2H), 3.41 (s, 2H), 3.36−3.32 (m, 2H), 2.48 (s, 8H), 2.38 (t, J = 6.6 Hz, 2H), 1.58−1.55 (m, 4H). ^{13}C NMR (100 MHz, $CDCl_3$) δ 192.60, 162.19, 147.62, 146.61, 131.93, 122.23, 109.49, 107.85, 100.87, 95.69, 85.73, 84.77, 62.68, 57.77, 53.18, 52.71, 39.49, 27.29, 24.03. TOF-ES$^+$-MS, $[M + H]^+$: m/z calcd for $C_{25}H_{29}N_3O_6{}^{185}Re$ 652.1586; found 652.1580.

*Pentafluorophenyl Ferrocenecarboxylate (**19**).* Ferrocenecarboxylic acid (501.5 mg, 2.18 mmol) and pentafluorophenyl trifluoroacetate (610.4 mg, 2.18 mmol) were dissolved in 2 mL of anhydrous DMF, and 100 μL of pyridine was added. The reaction mixture was stirred at room temperature for 4 h. The mixture was diluted with 30 mL of ethyl acetate and washed with 1 M HCl, saturated $NaHCO_3$, and saturated NaCl. The organic layer was then dried with anhydrous $MgSO_4$, filtered, concentrated under vacuum, and purified by silica gel column chromatography using petroleum ether as the mobile phase to afford **19** as an orange solid (494.7 mg, 57%); mp 75.5−77.0 °C. ^{1}H NMR (400 MHz, $CDCl_3$) δ 4.98 (t, J = 1.9 Hz, 2H), 4.59 (t, J = 1.9 Hz, 2H), 4.33 (s, 5H).

*3-(4-(1,3-Benzodioxol-5-ylmethyl)piperazin-1-yl)-propylcarbonylferrocene (**20**).* To a solution of **17** (300.0 mg, 0.89 mmol) in 4 mL of toluene and 4 mL of triethylamine, **9** (65.4 mg, 0.30 mmol) and KI (19.7 mg, 0.12 mmol) were added. The mixture was stirred at 115 °C in the dark for 4 h. After cooling to room temperature, the reaction mixture was concentrated under vacuum and purified by silica gel column chromatography using petroleum ether/triethylamine (10/1, v/v) as the mobile phase to afford **20** as an orange solid (84.5 mg, 60%); mp 82.1−84.1 °C. ^{1}H NMR (400 MHz, $CDCl_3$) δ 6.84 (s, 1H), 6.73 (s, 2H), 5.93 (s, 2H), 4.78 (t, J = 1.7 Hz, 2H), 4.48 (t, J = 1.7 Hz, 2H), 4.19 (s, 5H), 3.41 (s, 2H), 2.75 (t, J = 7.2 Hz, 2H), 2.47 (s, 8H), 2.43 (t, J = 7.3 Hz, 2H), 1.94−1.86 (m, 2H). ESI−MS, $[M + H]^+$ (m/z = 475.2).

*4-(4-(1,3-Benzodioxol-5-ylmethyl)piperazin-1-yl)-butylcarbonylferrocene (**21**).* The procedure described for the synthesis of **20** was applied to **18** to afford **21** as an orange oil (62%). ^{1}H NMR (400 MHz, $CDCl_3$) δ 6.84 (s, 1H), 6.73 (s, 2H), 5.93 (s, 2H), 4.78 (t, J = 1.8 Hz, 2H), 4.48 (t, J = 1.8 Hz, 2H), 4.19 (s, 5H), 3.41 (s, 2H), 2.72 (t, J = 7.3 Hz, 2H), 2.47 (s, 8H), 2.39 (t, J = 7.5 Hz, 2H), 1.76−1.68 (m, 2H), 1.61−1.53 (m, 2H). ESI−MS, $[M + H]^+$ (m/z = 488.9).

*2-(4-(1,3-Benzodioxol-5-ylmethyl)piperazin-1-yl)-ethylaminocarbonylferrocene (**22**).* To a solution of **19** (74.9 mg, 0.19 mmol) and **15a** (200.2 mg, 0.76 mmol) in anhydrous DMF, 200 μL of triethylamine was added. The reaction mixture was stirred at room temperature overnight. The solvent was then removed, and crude product was purified by silica gel column chromatography using ethyl acetate/petroleum ether/triethylamine (10/10/1, v/v/v) as the mobile phase to afford **22** as an orange solid (37.4 mg, 42%); mp 122.1−124.1 °C. ^{1}H NMR (400 MHz, $CDCl_3$) δ 6.84 (s, 1H), 6.75 (s, 2H), 5.95 (s, 2H), 4.81 (s, 2H), 4.35 (t, J = 1.8 Hz, 2H), 4.20 (s, 5H), 3.63 (s, 2H), 3.50 (s, 2H), 2.98−2.57 (m, 10H). ESI $[M + H]^+$ (m/z = 476.5).

In Vitro Radioligand Competition Studies. *σ Receptor Binding Assays.* All the procedures for the radioligand competition studies were previously described.[27] Detailed procedures are shown in the Supporting Information.

VAChT Binding Assays. Radioligand competition binding assays for VAChT were performed according to literature,[35] and detailed procedures are provided in the Supporting Information.

Radiochemistry. The ^{99m}Tc-pertechnetate was eluted from a commercial ^{99}Mo−^{99m}Tc generator obtained from Beijing Atomic High-Tech Co. The reactions were performed according to the method in the literature.[28,38] Detailed procedures are provided in the Supporting Information.

Measurement of log *D* Values. The log D values of [^{99m}Tc]**23**−**25** were determined by measuring the distribution of the radiotracer between 1-octanol and 0.05 mol·L^{-1} sodium phosphate buffer at pH 7.4 according to literature.[31] Detailed procedures are provided in the Supporting Information.

Biodistribution Studies in Mice and Blocking Studies. All animal experiments in ICR mice (n = 5, 4−5 weeks, 22−25 g) were performed in compliance with the national laws related to the care and experiments on laboratory animals. Biodistribution studies and blocking studies of HPLC-purified [^{99m}Tc]**23** or [^{99m}Tc]**24** (370 kBq in 0.1 mL saline) were carried out based on the method reported previously.[31] Detailed procedures are shown in the Supporting Information.

In Vivo Radiometabolic Stability of [^{99m}Tc]23. The in vivo metabolism of [^{99m}Tc]**23** (33 MBq, 0.15 mL) was studied in male ICR

dx.doi.org/10.1021/jm5009488 | J. Med. Chem. XXXX, XXX, XXX−XXX

mice according to the previously reported method.[49] Detailed procedures are shown in the Supporting Information.

Effect of P-gp on the Brain Uptake of [^{99m}Tc]23 in Mice. For the investigation of the effect of P-gp on the brain uptake of [^{99m}Tc]**23**, mice were injected via the tail vein with either saline (0.1 mL) or cyclosporine A (0.1 mL, 50.0 mg/kg) 60 min prior to [^{99m}Tc]**23** injection (370 kBq in 0.1 mL saline) according to the method in the literature.[50] Detailed information is provided in the Supporting Information.

In Vitro Uptake of [^{99m}Tc]23 in C6 Glioma Cell Lines. C6 glioma cells (Institute of Materia Medica, Chinese Academy of Medical Sciences and Peking Union Medical College, Beijing, China) were routinely grown as monolayers in RPMI-1640 medium (Macgene Biotech Co., Ltd., Beijing, China) supplemented with 10% (v) heat-inactivated fetal bovine serum (FBS) and antibiotics (100 U/mL penicillin and 100 μg/mL streptomycin) in an atmosphere containing 5% CO_2 at 37 °C.

Before each experiment, C6 glioma cells were seeded in the wells of 24-well plates. An equal number of cells (2×10^5 cells/well) was dispensed in each well and incubated with 1 mL of RPMI 1640 medium supplemented with 10% FBS overnight at 37 °C to allow firm adherence. For total binding experiments, 7.4 kBq of [^{99m}Tc]**23** in 1 mL of RPMI-1640 medium (50 μL of [^{99m}Tc]**23** in saline mixed with 0.95 mL of RPMI-1640 medium) was added to each well (in triplicate). For blocking studies, various concentrations of different competitors (2, 10, and 20 μM haloperidol; 2, 10, and 20 μM DTG; and 2, 10, and 20 μM SA4503) in 1 mL of RPMI-1640 medium with 7.4 kBq of [^{99m}Tc]**23** was added to each well (in triplicate). After 15, 30, or 60 min incubation at room temperature, the medium was quickly removed. The cells were rinsed twice with ice-cold phosphate-buffered saline containing 0.2% bovine serum albumin (BSA) and then lysed with 1 mL of NaOH (1 M) at room temperature. The cell-associated radioactivity was determined using a gamma counter (Wallac 1470 Wizard, PerkinElmer, USA). The administered [^{99m}Tc]**23** (7.4 kBq) in each well was used as the administered tracer dose. The cell uptake (%) of [^{99m}Tc]**23** was calculated by the formula: Uptake (%) = counts per minute (CPM) (in the cell suspension)/CPM (administered tracer dose) × 100%.

The %blocking was calculated by [(radioactivity accumulation under blocking condition) − (radioactivity accumulation under control condition)]/(radioactivity accumulation under control condition) × 100%. Significant differences between control and blocking groups were determined by Student's *t* test (independent, two-tailed). The criterion for significance was $p \leq 0.05$.

In Vitro Uptake of [^{99m}Tc]23 in DU145 Prostate Cell Lines. DU145 prostate cells (National Platform of Experimental Cell Resources for Sci-Tech) were routinely grown as monolayers in RPMI-1640 medium (Macgene Biotech Co., Ltd., Beijing, China) supplemented with 10% (v) heat-inactivated FBS and 1% (v) antibiotics (100 U/mL penicillin and 100 μg/mL streptomycin) in an atmosphere containing 5% CO_2 at 37 °C.

The in vitro cell uptake experiments were performed with the method described above. For total binding experiments, 7.4 kBq of [^{99m}Tc]**23** was added in 1 mL of RPMI-1640 medium (50 μL of radioligand in saline mixed with 0.95 mL RPMI-1640 medium) was added to each well (in triplicate). For blocking studies, various concentrations of SA4503 (10^{-11}, 10^{-10}, 10^{-9}, 10^{-8}, 10^{-7}, 10^{-6}, 10^{-5}, 10^{-4}, and 10^{-3} M) in 1 mL of RPMI-1640 medium with 7.4 kBq of radioligand was added to each well (in triplicate). After 60 min incubation at room temperature, the medium was quickly removed. The cells were rinsed twice with ice-cold phosphate-buffered saline containing 0.2% BSA and then lysed with 1 mL of NaOH (1 M) at room temperature. The cell-associated radioactivity was measured using a gamma counter (Wallac 1470 Wizard, PerkinElmer, USA). The administered radioligand (7.4 kBq) in each well was used as the administered tracer dose.

The percentage of cell uptake (uptake (%)) and %blocking were calculated as described above.

Blocking Studies in C6 Glioma Tumor-Bearing Mice. ICR mice were purchased from Peking University Health Science Center at 4 weeks of age. Animals were housed under standard conditions with free access to food and water. All of the animal experiments adhered to the principles of care and use of laboratory animals and were approved by the Institutional Animal Care and Use Committee of Peking University.

C6 glioma cells were routinely grown as monolayers. After harvesting these cells, C6 glioma cells were diluted with serum-free RPMI-1640 medium to achieve a cell concentration of 5×10^7/mL. A 100 μL cell suspension was implanted subcutaneously in the scapular region of ICR mice (4−5 weeks old). The biodistribution studies were performed 7−10 days after implantation when the tumor size was approximately 0.2 cm^3 (approximately 200 mg).

Blocking studies in C6 tumor-bearing mice ($n = 5$) were conducted by injecting 1.0 mg/kg haloperidol (0.1 mL) or 3 μM DTG (0.1 mL) 5 min prior to [^{99m}Tc]**23** injection. The animals were sacrificed at 60 min postinjection. Samples of the blood, brain, heart, liver, spleen, lung, kidneys, muscle, and tumor were isolated and analyzed as described above. Significant differences between control and blocking groups were determined by Student's *t* test (independent, two-tailed). The criterion for significance was $p \leq 0.05$.

■ ASSOCIATED CONTENT

Supporting Information

General information and some parts of evaluation of the radiotracers in the Experimental Section, purity of key target compounds, the HPLC analysis of lipophilicity of rhenium complexes **10a** and **16a**, and the HPLC coinjection profiles of [^{99m}Tc]**23** and **10a**, [^{99m}Tc]**24** and **10b**, [^{99m}Tc]**25** and **16a**. This material is available free of charge via the Internet at http://pubs.acs.org.

■ AUTHOR INFORMATION

Corresponding Author

*Phone: +86-10-58808891. Fax: +86-10-58808891. E-mail: hmjia@bnu.edu.cn.

Notes

The authors declare no competing financial interest.

■ ACKNOWLEDGMENTS

This work was supported by the National Natural Science Foundation of China (no. 21071023).

■ ABBREVIATIONS USED

AD, Alzheimer's disease; BSA, bovine serum albumin; CNS, central nervous system; CPM, counts per minute; DLT, double ligand transfer; DMF, dimethylformamide; DTG, 1,3-di-*o*-tolylguanidine; FBS, fetal bovine serum; HPLC, high performance liquid chromatography; ID, injected dose; PD, Parkinson's disease; PET, positron emission tomography; P-gp, permeability-glycoprotein; rt, room temperature; SD, standard deviation; SPECT, single photon emission computed tomography; TFA, trifluoroacetic acid; THF, tetrahydrofuran; TLC, thin layer chromatography; VAChT, vesicular acetylcholine transporter

■ REFERENCES

(1) Hayashi, T.; Su, T.-P. Sigma-1 receptor chaperones at the ER-mitochondrion interface regulate Ca^{2+} signaling and cell survival. *Cell* **2007**, *131*, 596−610.

(2) Hanner, M.; Moebius, F. F.; Flandorfer, A.; Knaus, H.-G.; Striessnig, J.; Kempner, E.; Glossmann, H. Purification, molecular cloning, and expression of the mammalian sigma1-binding site. *Proc. Natl. Acad. Sci. U. S. A.* **1996**, *93*, 8072−8077.

(3) Aydar, E.; Palmer, C. P.; Klyachko, V. A.; Jackson, M. B. The sigma receptor as a ligand-regulated auxiliary potassium channel subunit. *Neuron* **2002**, *34*, 399−410.
(4) Maurice, T.; Su, T.-P. The pharmacology of sigma-1 receptors. *Pharmacol. Ther.* **2009**, *124*, 195−206.
(5) Hayashi, T.; Tsai, S.-Y.; Mori, T.; Fujimoto, M.; Su, T.-P. Targeting ligand-operated chaperone sigma-1 receptors in the treatment of neuropsychiatric disorders. *Expert Opin. Ther. Targets* **2011**, *15*, 557−577.
(6) Kourrich, S.; Su, T.-P.; Fujimoto, M.; Bonci, A. The sigma-1 receptor: roles in neuronal plasticity and disease. *Trends Neurosci.* **2012**, *35*, 762−771.
(7) Fehér, Á.; Juhász, A.; László, A.; Kálmán, J., Jr.; Pákáski, M.; Kálmán, J.; Janka, Z. Association between a variant of the sigma-1 receptor gene and Alzheimer's disease. *Neurosci. Lett.* **2012**, *517*, 136−139.
(8) Uchida, N.; Ujike, H.; Tanaka, Y.; Sakai, A.; Yamamoto, M.; Fujisawa, Y.; Kanzaki, A.; Kuroda, S. A variant of the sigma receptor type-1 gene is a protective factor for Alzheimer disease. *Am. J. Geriatr. Psychiatry* **2005**, *13*, 1062−1066.
(9) Mishina, M.; Ishiwata, K.; Ishii, K.; Kitamura, S.; Kimura, Y.; Kawamura, K.; Oda, K.; Sasaki, T.; Sakayori, O.; Hamamoto, M. Function of sigma1 receptors in Parkinson's disease. *Acta Neurol. Scand.* **2005**, *112*, 103−107.
(10) Bermack, J. E.; Debonnel, G. The role of sigma receptors in depression. *J. Pharmacol. Sci.* **2005**, *97*, 317−336.
(11) Fishback, J. A.; Robson, M. J.; Xu, Y.-T.; Matsumoto, R. R. Sigma receptors: potential targets for a new class of antidepressant drug. *Pharmacol. Ther.* **2010**, *127*, 271−282.
(12) Wang, B.; Rouzier, R.; Albarracin, C.; Sahin, A.; Wagner, P.; Yang, Y.; Smith, T.; Bernstam, F. M.; Marcelo, A. C.; Hortobagyi, G. Expression of sigma1 receptor in human breast cancer. *Breast Cancer Res. Treat.* **2004**, *87*, 205−214.
(13) Vilner, B. J.; John, C. S.; Bowen, W. D. Sigma-1 and sigma-2 receptors are expressed in a wide variety of human and rodent tumor cell lines. *Cancer Res.* **1995**, *55*, 408−413.
(14) van Waarde, A.; Rybczynska, A. A.; Ramakrishnan, N. K.; Ishiwata, K.; Elsinga, P. H.; Dierckx, R. A.J.O. Sigma receptors in oncology: therapeutic and diagnostic applications of sigma ligands. *Curr. Pharm. Des.* **2010**, *16*, 3519−3537.
(15) Megalizzi, V.; Le Mercier, M.; Decaestecker, C. Sigma receptors and their ligands in cancer biology: overview and new perspectives for cancer therapy. *Med. Res. Rev.* **2012**, *32*, 410−427.
(16) Megalizzi, V.; Decaestecker, C.; Debeir, O.; Spiegl-Kreinecker, S.; Berger, W.; Lefranc, F.; Kast, R. E.; Kiss, R. Screening of anti-glioma effects induced by sigma-1 receptor ligands: potential new use for old anti-psychiatric medicines. *Eur. J. Cancer* **2009**, *45*, 2893−2905.
(17) Brust, P.; Deuther-Conrad, W.; Lehmkuhl, K.; Jia, H.; Wuensch, B. Molecular imaging of σ_1 receptors in vivo: current status and perspectives. *Curr. Med. Chem.* **2014**, *21*, 35−69.
(18) Waterhouse, R. N.; Chang, R. C.; Atuehene, N.; Collier, T. L. In vitro and in vivo binding of neuroactive steroids to the sigma-1 receptor as measured with the positron emission tomography radioligand [^{18}F] FPS. *Synapse* **2007**, *61*, 540−546.
(19) Stone, J. M.; Årstad, E.; Erlandsson, K.; Waterhouse, R. N.; Ell, P. J.; Pilowsky, L. S. [^{123}I]TPCNE—a novel SPET tracer for the sigma-1 receptor: first human studies and in vivo haloperidol challenge. *Synapse* **2006**, *60*, 109−117.
(20) Ishikawa, M.; Ishiwata, K.; Ishii, K.; Kimura, Y.; Sakata, M.; Naganawa, M.; Oda, K.; Miyatake, R.; Fujisaki, M.; Shimizu, E.; Shirayama, Y.; Iyo, M.; Hashimoto, K. High occupancy of sigma-1 receptors in the human brain after single oral administration of fluvoxamine: a positron emission tomography study using [^{11}C]-SA4503. *Biol. Psychiatry* **2007**, *62*, 878−883.
(21) Ishikawa, M.; Sakata, M.; Ishii, K.; Kimura, Y.; Oda, K.; Toyohara, J.; Wu, J.; Ishiwata, K.; Iyo, M.; Hashimoto, K. High occupancy of σ_1 receptors in the human brain after single oral administration of donepezil: a positron emission tomography study using [^{11}C]SA4503. *Int. J. Neuropsychopharmacol.* **2009**, *12*, 1127−1131.
(22) Sakata, M.; Kimura, Y.; Naganawa, M.; Oda, K.; Ishii, K.; Chihara, K.; Ishiwata, K. Mapping of human cerebral sigma$_1$ receptors using positron emission tomography and [^{11}C]SA4503. *NeuroImage* **2007**, *35*, 1−8.
(23) Johannsen, B.; Pietzsch, H.-J. Development of technetium-99m-based CNS receptor ligands: have there been any advances? *Eur. J. Nucl. Med. Mol. Imaging* **2002**, *29*, 263−275.
(24) Satpati, D.; Bapat, K.; Sarma, H. D.; Venkatesh, M.; Banerjee, S. Synthesis, characterization and biological activity of ^{99m}Tc-labeled piperidine analogues targeting sigma receptors. *J. Labelled Compd. Radiopharm.* **2010**, *53*, 198−204.
(25) Friebe, M.; Mahmood, A.; Bolzati, C.; Drews, A.; Johannsen, B.; Eisenhut, M.; Kraemer, D.; Davison, A.; Jones, A. G. [^{99m}Tc]-oxotechnetium(V) complexes of amine-amide-dithiol chelates with dialkylaminoalkyl substituents as potential diagnostic probes for malignant melanoma. *J. Med. Chem.* **2001**, *44*, 3132−3140.
(26) Lu, J.; Kong, D.; Jia, H.; Deuther-Conrad, W.; Brust, P.; Wang, X. Preparation and biological evaluation of ^{99m}TcN-4-(cyclohexylpiperazin-1-yl)-dithioformate as a potential sigma receptor imaging agent. *J. Labelled Compd. Radiopharm.* **2007**, *50*, 1200−1205.
(27) Fan, C.; Jia, H.; Deuther-Conrad, W.; Brust, P.; Steinbach, J.; Liu, B. Novel ^{99m}Tc labeled σ receptor ligand as a potential tumor imaging agent. *Sci. China, Ser. B: Chem.* **2006**, *49*, 169−176.
(28) Chen, X.; Cui, M. C.; Deuther-Conrad, W.; Tu, Y. F.; Ma, T.; Xie, Y.; Jia, B.; Li, Y.; Xie, F.; Wang, X.; Steinbach, J.; Brust, P.; Liu, B. L.; Jia, H. M. Synthesis and biological evaluation of a novel ^{99m}Tc cyclopentadienyl tricarbonyl complex ([(Cp-R)^{99m}Tc(CO)$_3$]) for sigma-2 receptor tumor imaging. *Bioorg. Med. Chem. Lett.* **2012**, *22*, 6352−6357.
(29) John, C. S.; Lim, B. B.; Geyer, B. C.; Vilner, B. J.; Bowen, W. D. ^{99m}Tc-labeled σ-receptor-binding complex: synthesis, characterization, and specific binding to human ductal breast carcinoma (T47D) cells. *Bioconjugate Chem.* **1997**, *8*, 304−309.
(30) Alberto, R.; Abram, U. ^{99m}Tc: labeling chemistry and labeled compounds. In *Handbook of Nuclear Chemistry*, 2nd ed.; Vértes, A., Nagy, S., Klencsár, Z., Lovas, R. G., Rösch, F., Eds.; Springer: New York, 2011, Vol. *4*; pp 2073−2120.
(31) Wang, X.; Li, Y.; Deuther-Conrad, W.; Xie, F.; Chen, X.; Cui, M.-C.; Zhang, X.-J.; Zhang, J.-M.; Steinbach, J.; Brust, P.; Liu, B.-L.; Jia, H.-M. Synthesis and biological evaluation of ^{18}F labeled fluoro-oligo-ethoxylated 4-benzylpiperazine derivatives for sigma-1 receptor imaging. *Bioorg. Med. Chem.* **2013**, *21*, 215−222.
(32) Glennon, R. Pharmacophore identification for sigma-1 (σ_1) receptor binding: application of the "deconstruction−reconstruction−elaboration" approach. *Mini-Rev. Med. Chem.* **2005**, *5*, 927−940.
(33) N'Dongo, H. P.; Liu, Y.; Can, D.; Schmutz, P.; Spingler, B.; Alberto, R. Aqueous syntheses of [(Cp-R)M(CO)$_3$] type complexes (Cp = cyclopentadienyl, M = Mn, ^{99m}Tc, Re) with bioactive functionalities. *J. Organomet. Chem.* **2009**, *694*, 981−987.
(34) Reynaud, P.; Brion, J.; Nguyentrixuong, E.; Davrinche, C.; Pieri, F.; Arnouldguerin, M. Anti-atthythmic agents related to procainamide II. Synthesis and pharmacological study. *Eur. J. Med. Chem.* **1989**, *24*, 427−434.
(35) Sorger, D.; Scheunemann, M.; Großmann, U.; Fischer, S.; Vercouille, J.; Hiller, A.; Wenzel, B.; Roghani, A.; Schliebs, R.; Brust, P.; Sabri, O.; Steinbach, J. A new ^{18}F-labeled fluoroacetylmorpholino derivative of vesamicol for neuroimaging of the vesicular acetylcholine transporter. *Nucl. Med. Biol.* **2008**, *35*, 185−195.
(36) Cesati, R. R.; Tamagnan, G.; Baldwin, R. M.; Zoghbi, S. S.; Innis, R. B.; Kula, N. S.; Baldessarini, R. J.; Katzenellenbogen, J. A. Synthesis of cyclopentadienyltricarbonyl rhenium phenyltropanes by double ligand transfer: organometallic ligands for the dopamine transporter. *Bioconjugate Chem.* **2002**, *13*, 29−39.
(37) Štěpnička, P.; Verníček, M.; Schulz, J.; Císařová, I. Synthesis and structural characterization of a sterically encumbered ferrocenecarboxamido diphosphine and its platinum(II) complex. *J. Organomet. Chem.* **2014**, *755*, 41−46.

(38) Saidi, M.; Kothari, K.; Pillai, M.; Hassan, A.; Sarma, H.; Chaudhari, P.; Unnikrishnan, T.; Korde, A.; Azzouz, Z. Cyclopentadienyl technetium (^{99m}Tc) tricarbonyl piperidine conjugates: biodistribution and imaging studies. *J. Labelled Compd. Radiopharm.* **2001**, *44*, 603−618.
(39) Chen, R.-Q.; Li, Y.; Zhang, Q.-Y.; Jia, H.-M.; Deuther-Conrad, W.; Schepmann, D.; Steinbach, J.; Brust, P.; Wünsch, B.; Liu, B.-L. Synthesis and biological evaluation of a radioiodinated spiropiperidine ligand as a potential σ_1 receptor imaging agent. *J. Labelled Compd. Radiopharm.* **2010**, *53*, 569−574.
(40) Kreisl, W. C.; Liow, J. S.; Kimura, N.; Seneca, N.; Zoghbi, S. S.; Morse, C. L.; Herscovitch, P.; Pike, V. W.; Innis, R. B. P-glycoprotein function at the blood−brain barrier in humans can be quantified with the substrate radiotracer ^{11}C-*N*-desmethyl-loperamide. *J. Nucl. Med.* **2010**, *51*, 559−566.
(41) Mishina, M.; Ohyama, M.; Ishii, K.; Kitamura, S.; Kimura, Y.; Oda, K.; Kawamura, K.; Sasaki, T.; Kobayashi, S.; Katayama, Y.; Ishiwata, K. Low density of sigma$_1$ receptors in early Alzheimer's disease. *Ann. Nucl. Med.* **2008**, *22*, 151−156.
(42) Li, Z. J.; Ren, H. Y.; Cui, M. C.; Deuther-Conrad, W.; Tang, R. K.; Steinbach, J.; Brust, P.; Liu, B. L.; Jia, H. M. Synthesis and biological evaluation of novel 4-benzylpiperazine ligands for sigma-1 receptor imaging. *Bioorg. Med. Chem.* **2011**, *19*, 2911−2917.
(43) Patel, S.; Gibson, R. In vivo site-directed radiotracers: a mini-review. *Nucl. Med. Biol.* **2008**, *35*, 805−815.
(44) Meegalla, S. K.; Plössl, K.; Kung, M.-P.; Chumpradit, S.; Stevenson, D. A.; Kushner, S. A.; McElgin, W. T.; Mozley, P. D.; Kung, H. F. Synthesis and characterization of technetium-99m-labeled tropanes as dopamine transporter-imaging agents. *J. Med. Chem.* **1997**, *40*, 9−17.
(45) Yamazaki, M.; Neway, W. E.; Ohe, T.; Chen, I.-W.; Rowe, J. F.; Hochman, J. H.; Chiba, M.; Lin, J. H. In vitro substrate identification studies for P-glycoprotein-mediated transport: species difference and predictability of in vivo results. *J. Pharmacol. Exp. Ther.* **2001**, *296*, 723−735.
(46) John, C. S.; Vilner, B. J.; Geyer, B. C.; Moody, T.; Bowen, W. D. Targeting sigma receptor-binding benzamides as in vivo diagnostic and therapeutic agents for human prostate tumors. *Cancer Res.* **1999**, *59*, 4578−4583.
(47) Bowen, W. D.; Moses, E. L.; Tolentino, P. J.; Walker, J. M. Metabolites of haloperidol display preferential activity at sigma receptors compared to dopamine D-2 receptors. *Eur. J. Pharmacol.* **1990**, *177*, 111−118.
(48) Matsuno, K.; Nakazawa, M.; Okamoto, K.; Kawashima, Y.; Mita, S. Binding properties of SA4503, a novel and selective σ_1 receptor agonist. *Eur. J. Pharmacol.* **1996**, *306*, 271−279.
(49) Li, Y.; Wang, X.; Zhang, J.; Deuther-Conrad, W.; Xie, F.; Zhang, X.; Liu, J.; Qiao, J.; Cui, M.; Steinbach, J.; Brust, P.; Liu, B.; Jia, H. Synthesis and evaluation of novel ^{18}F-labeled spirocyclic piperidine derivatives as σ_1 receptor ligands for positron emission tomography imaging. *J. Med. Chem.* **2013**, *56*, 3478−3491.
(50) Li, Z.; Cui, M.; Dai, J.; Wang, X.; Yu, P.; Yang, Y.; Jia, J.; Fu, H.; Ono, M.; Jia, H.; Saji, H.; Liu, B. Novel cyclopentadienyl tricarbonyl complexes of ^{99m}Tc mimicking chalcone as potential single-photon emission computed tomography imaging probes for beta-amyloid plaques in brain. *J. Med. Chem.* **2013**, *56*, 471−482.